Elsevier Editorial System(tm) for Materials and Design

Manuscript Draft

Manuscript Number: JMAD-D-18-00607R3

Title: ANN prediction of corrosion behaviour of uncoated and biopolymers coated cp-Titanium substrates.

Article Type: Research Paper

Keywords: cp-Ti, Chitosan, Gelatin, Sodium Alginate, Electrochemical Impedance Spectroscopy (EIS), Artificial Neural Network (ANN)

Corresponding Author: Dr. Suman Kumari, Ph.D

Corresponding Author's Institution: Ghent University.Belgium

First Author: Suman Kumari

Order of Authors: Suman Kumari; Hanuma R Tiyyagura, Ph.D; Timothy Douglas; Elbeshary Mohammed; Annemie Adriaens; Regina fuchs-Godec; Krishna Mohan Matravadi; Andre Skirtach

Abstract: The present study focuses on biopolymer surface modification of cp-Titanium with Chitosan, Gelatin and Sodium Alginate. The biopolymers were spin coated onto cp-Titanium substrate and further subjected to Electrochemical Impedance Spectroscopic (EIS) characterisation. Artificial Neural Network (ANN) was developed to predict the Open Cicuit Potential (OCP) values and Nyquist plot for bare and bioploymer coated cp-Titanium substrate. The experimental data obtained was utilised for ANN training. Two input paramters, i.e., substrate condition (coated or uncoated) and time period were considered to predict the OCP values. Back propogation Levenberg-Marquardt training algorithm was utilised in order to train ANN and to fit the model. For Nyquist plot, the network was trained to predict the imaginary impedance based on real impedance as a function of immersion periods using the Back Propagation Bayesian algorithm. The biopolymer coated cp-Titanium substrate shows the enhanced corrosion resistance compared to uncoated substrtaes. The ANN model exhibits excellent comparsion with the experimental results in both the cases indicating that the developed model is very accurate and efficiently predicts the OCP values and Nyquist plot.

Suman Kumari
Department of Metallurgical and Material Enginnering,
National Institute of Technology(NIT) Warangal,
Warangal,
India.
Email: suman.shakya15@gmail.com

Warangal, India 30.6.2018

Dear Editor,

Please find attached a revised manuscript (third time) with the title: "***ANN prediction of corrosion behaviour of uncoated and biopolymers coated cp-Titanium substrates***".

First of all, we would like to thank you for your comments for the improvement of our manuscript. Following these comments, we have corrected the comments, and uploaded a manuscript with modified graphical abstract and highlights. The answers to the questions and comments raised can be found in the response to decision letter. We hope that you will now find our contribution suitable to be published as an article in *Materials &Design.*

With kind regards

Suman Kumari.

Comments from the editors and reviewers:

Comments:

Editorial:

The graphical abstract and highlights should be revised according to recently published guidelines: http://www.sciencedirect.com/science/article/pii/S0264127515005031
In addition, more than 25% of the references should be from the last three years (2016-2018), in order to show the potential impact of this paper on the relevant fields for Materials & Design.

Answer: Dear Editor, the graphical abstract, highlights and references revised as suggested.

*Graphical Abstract

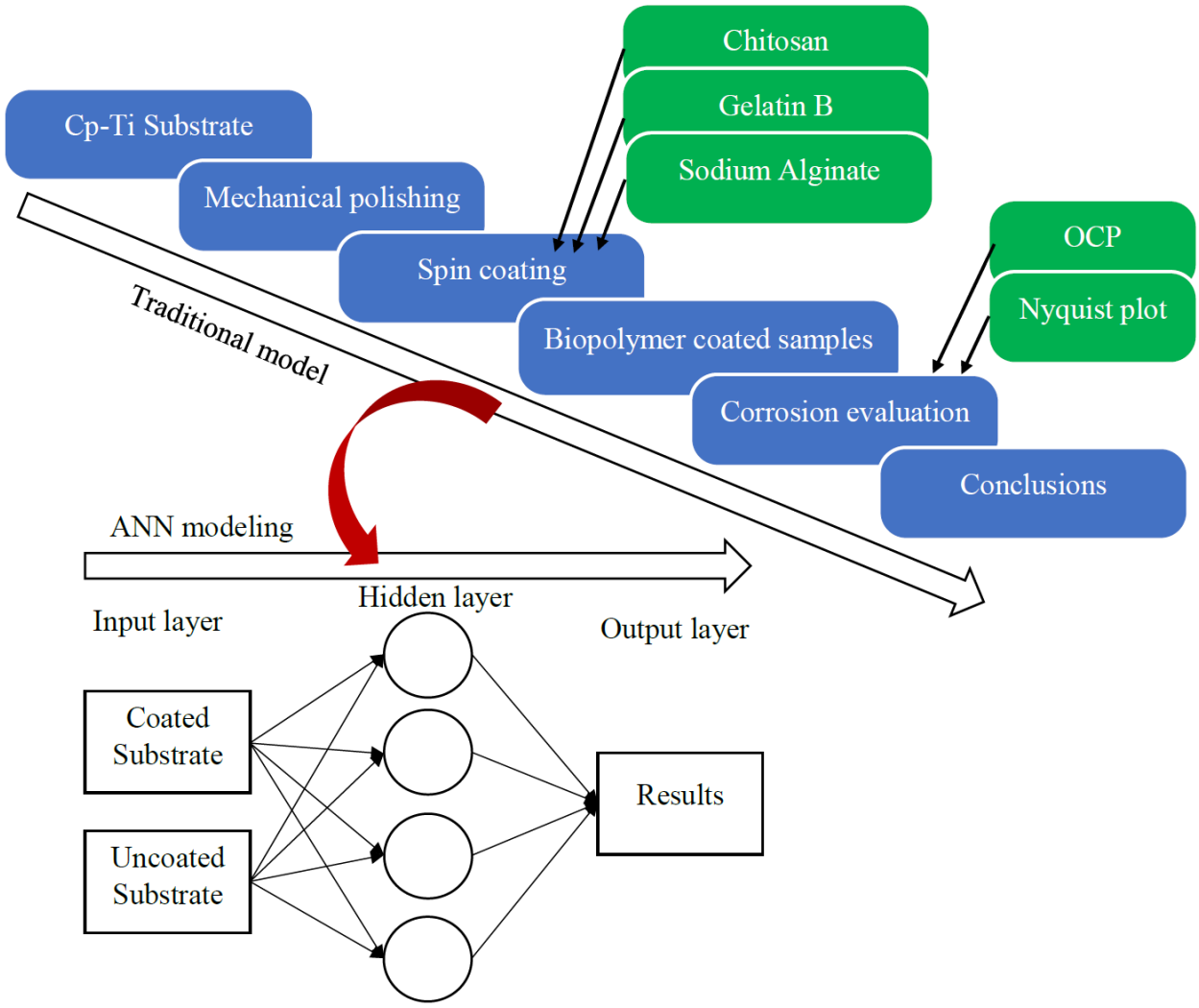

Highlights

- The present study focuses on evaluation of corrosion behaviour of uncoated and biopolymer coated commercially pure (CP) Ti.
- Three biopolymers, *i.e.*, Chitosan, Gelatin B and Sodium Alginate were coated *via*. spin coating technique.
- Open Circuit Potential (OCP) and Electrochemical Impedance spectroscopy (EIS) studies were carried out for corrosion evaluation.
- Artificial Neural Network (ANN) modeling is carried out to predict OCP values and Nyquist plots.
- Sodium Alginate coated Ti substrates shows the highest corrosion resistance among all three biopolymers.
- The present ANN model can be used to predict OCP values and Nyquist plots accurately.

ANN prediction of corrosion behaviour of uncoated and biopolymers coated cp-Titanium substrates

Suman Kumari[a*], Hanuma Reddy Tiyyagura[b], Timothy E. L. Douglas[c], Elbeshary A. A. Mohammed[d], Annemie Adriaens[d], Regina fuchs-Godec[b], M. K. Mohan[a] and Andre Skiratch[c,f]

[a]Dept. of Metallurgical and Materials Engineering, National Institute of Technology Warangal, India

[b] Faculty of Chemistry and Chemical Engineering, University of Maribor, Maribor, Slovenia

[c]Dept. of Molecular Biotechnology, Ghent University, Belgium

[d]Dept. of Analytical Chemistry, Ghent University, Belgium

[f] Centre for Nano- and Biophotonics, Ghent University, Belgium

Corresponding author: *suman.shakya15@gmail.com

Abstract

The present study focuses on biopolymer surface modification of cp-Titanium with Chitosan, Gelatin, and Sodium Alginate. The biopolymers were spin coated onto a cp-Titanium substrate and further subjected to Electrochemical Impedance Spectroscopic (EIS) characterization. Artificial Neural Network (ANN) was developed to predict the Open Circuit Potential (OCP) values and Nyquist plot for bare and biopolymer coated cp-Titanium substrate. The experimental data obtained was utilized for ANN training. Two input parameters, i.e., substrate condition (coated or uncoated) and time period were considered to predict the OCP values. Backpropagation Levenberg-Marquardt training algorithm was utilized in order to train ANN and to fit the model. For Nyquist plot, the network was trained to predict the imaginary impedance based on real impedance as a function of immersion periods using the Back Propagation Bayesian algorithm. The biopolymer coated cp-Titanium substrate shows the enhanced corrosion resistance compared to uncoated substrates. The ANN model exhibits excellent comparison with the experimental results in both the cases indicating that the developed model is very accurate and efficiently predicts the OCP values and Nyquist plot.

Keywords: cp-Ti, Chitosan, Gelatin, Sodium Alginate, Electrochemical Impedance Spectroscopy (EIS), Artificial Neural Network (ANN).

1. Introduction

Metallic materials continue to dominate the biomedical industry, especially for hard tissue replacement (orthopaedic, dental) and cardiac implants[1],[2],[3]. A broad range of metals are known to mankind, but among them only a few are suitable for using inside the human body. The main factors contributing towards the selection of a metal for the orthopaedic implants are biocompatibility, should have adequate mechanical properties and must be corrosion resistant[4]. Titanium and Titanium alloys have emerged as materials of choice for biomedical implant applications [5],[6],[7],[8],[9],[10],[11]. CP-Ti (Commercially pure Titanium) and Ti-6Al-4V (ELI) Titanium-6 Vanadium-4 Aluminum (Extra Low Interstitial) are the two most common base implant materials[12],[13],[14],[15]. However, these alloys have certain disadvantages such as poor osseointegration properties and low corrosive-wear resistance[10],[16]. The surface coating of implant with organic polymer is an effective and inexpensive strategy to improve the corrosion behaviour and biocompatibility of the substrate surface[17]. Numerous biopolymers have been coated to evaluate the surface response of the substrate. Corrosion is an important aspect for a biomaterial due to extreme corrosive nature of the human body fluids[18]. The corrosion deterioration can reduce the lifespan of implant leading to need to revision surgery[19]. The Ti and Ti alloys are characterized by instantaneously formed stable oxide layer which is responsible for their exceptional corrosion resistance[20]. But once the stable TiO_2 is broken down or removed, it is unable to reform on parts of surface. Thus, making Ti implants susceptible to corrosion. The studies have also suggested that cp-Ti undergoes stress corrosion cracking (SCC) , severe form of corrosion, in the presence of fluoride ions[21]. Many surface modification has been used to modify the surface to enhance corrosion resistance of the implants. In this regard, surface coatings with biopolymer is an easy and inexpensive technique[18].

A considerable amount of research has been focussed towards functionalization of the implant with Chitosan(CS)[22]. CS is a cationic polysaccharide and deacetylated derivative of Chitin[23],[24], [25],[26].[27] CS is a nontoxic polymer which assists in wound healing and promotes osteogenesis[28]. CS is used for biomedical applications in many forms, such as scaffolds[29],[30],[31] and as hydrogels[32],[33],[34] Sodium Alginate (SA) is another natural biodegradable polysaccharide[35],[36], exhibiting biocompatibility, bio-functionality, non-toxicity and low cost[35]. SA, as a component of multilayer assembly, is being coated on a number of substrates[37],[38],[39]. On the other hand, Gelatin (Gel) is a water-soluble, biodegradable polypeptide, derived from collagen by partial synthesis [40]. Collagen is one of the key structural protein found in the extracellular matrix of many connective tissues. Over the years, Gel is utilized for many applications ranging from the food industry to pharmaceuticals[41]. Gel coated Titanium substrate showed the enhanced cell biocompatibility and cell adhesion and growth[42].

Artificial Neural Network (ANN) is a computational tool based on biological neural network system[43]. ANN is a powerful mathematical tool to simulate a wide variety of complex scientific and engineering problems ANN prediction is useful in many applications in engineering and applied sciences like biomedical applications[44],food science [45],solar cell systems [46],[47],energy systems[48],communication systems [49],nuclear materials[50]. Many attempts have been made in order to imply ANN in different fields for a number of applications, like speech recognition[51],[52], prediction of coating thickness[53], prediction of mechanical properties[54],[55], weather prediction[56], pharmaceutical research[57], identification of cell behaviour[58], medical imaging[59], predicting corrosion behaviour[60],[61],[62] *etc*.

In the present work, uncoated and biopolymer coated cp-Ti are characterized for evaluation

of their corrosion behaviour. Evaluation and quantification of corrosion process are time-consuming and in case of the implant materials, it is difficult to monitor the corrosion process on a real-time basis. In this regard, ANN is a potential technique which can be used to predict the corrosion rate in presence of corrosive human body fluids. Further, the implant failure can be estimated based on corrosion behaviour.

The OCP (Open Circuit Potential) studies were carried out on uncoated and coated substrates. EIS studies were also performed to obtain Nyquist plots to determine corrosion behaviour. The input database was prepared based on experimental studies[63],[64]. Artificial Neural Network (ANN) was trained to utilize the experimental database for predicting the corrosion behaviour of coated and uncoated Ti substrate with Open Circuit Potential (OCP) values and Nyquist plot.

2. Experimental Procedure

2.1. Materials and Methods

CP-Ti foil with thickness 0.125 mm was procured (Goodfellow UK). The samples with the dimension 1 cm X 1 cm were cut and further polished with SiC paper (up to 1200 grade) to remove the native oxide. The polished samples were cleaned ultrasonically in acetone followed by ethanol for 15 mins respctively. CS (DA 75%-85%), Gel B and SA were purchased from Sigma Aldrich. Analytical grade reagents were used without further purification. Phosphate Buffered Saline (PBS) was prepared by dissolving PBS tablet in Deionized water (dissolving one PBS tablet in 200 mL of DI water resulted in 0.01M PBS solution).

2.2. Biopolymer coating

The polished and cleaned samples were subjected to spin coating. 1 wt% CS solution, 10 wt% Gel (Type B) and 3 wt% SA were prepared by dissolving in deionized water. The samples were spin coated at 4000 rpm with 2500 rpm/s acceleration for a time period of 60 seconds.

2.3. Attenuated total reflection-Fourier Transform Infrared (ATR-FTIR) spectroscopy analysis

ATR-FTIR spectroscopy analysis of the substrates were performed to identify the presence of all three biopolymers onto the surface before and after incubation for 24 hours in PBS by Perkin-Elmer IR spectrophotometer with a Golden Gate attenuated total reflection (ATR) attachment with a diamond crystal. The spectra were accumulated within 16 scans at a resolution of 4 cm^{-1} within a range of 4000 cm^{1} to 650 cm^{-1}. The background air spectrum was subtracted before each measurement.

2.4. Surface characterization

The surface morphology of the coated samples after incubation for 24 hours was examined with Scanning electron microscope (FEI Quanta 200 3D).

2.5. Electrochemical characterization

Electrochemical experiments were performed with a conventional three-electrode configuration (Solartron 1287 Electrochemical interface with a Gamry 600™ potentiostat/galvanostat) with substrate as working electrode, Platinum as counter electrode and SCE (Saturated Calomel Electrode) as reference electrode. All experiments were carried out at room temperature. The test specimens were fixed in a PTFE holder exposing 1 cm^2

area to the electrolyte. The prepared PBS solution was used as electrolyte for all measurements.

2.6. Artificial Neural Network (ANN) Modelling

2.6.1. OCP Prediction

To develop the ANN model, the experimental data was randomly divided into three parts, training dataset (70%), testing dataset (15%) and validation dataset (15%). Back Propagation Levenberg-Marquardt (BPLM) training algorithm, supervised learning technique, was utilised in order to train the ANN and fit the model. The BPLM algorithm calculates the root mean square error (RMSE) with theoretical values and network prediction. NN linear transfer function was used for transforming neuron input value into the output values. The transfer function for the hidden layers was sigmoidal. Two inputs, *i.e.*, condition of the substrate (uncoated or coated) and different time period, were taken into consideration. Thus, the architecture of ANN becomes 2-20-1. One hidden layer with 20 neurons was found to be optimum. The NN presented for the given problem was created using MATLAB r2016a. Parameters affecting the OCP values were considered as inputs, i.e., sample condition and immersion time. The network was then trained to predict the OCP values. The input dataset was normalised (unity based normalization) to obtain the values ranging from 0 to 1 (equation 10).

$$x = (xi - xmin)/(xmax - xmin) \quad (10)$$

2.6.2. Nyquist plot prediction

The experimental database was divided randomly into training data set (80%) and testing dataset (20%). Backpropagation Bayesian (BPB) algorithm updates the weight and bias values according to the Levenberg-Marquardt optimization. Bayesian regularization

minimizes the initial combination of squared errors and weights and then determines the correct combination so as to produce a network that generalizes well[65]. The real and imaginary impedance values were the inputs for ANN. Based on these two inputs, the imaginary impedance values for uncoated and biopolymer coated Ti are predicted. The ANN architecture is 2-20-1, with optimum results showing for one hidden layer with 20 neurons. The pseudo code for prediction of corrosion parameters for the Nyquist plot is shown in Figure 1.

3. Results and Discussion

3.1. ATR-FTIR measurements

FTIR spectra of CS coated Ti are shown in Figure 2. The characteristic absorption peak at wavelength 3309 cm^{-1} is vibration of O-H (3000 cm^{-1}-3750 cm^{-1}) and N-H (3000 cm^{-1}-3750 cm^{-1}) bands[66]. The peaks at 2901 and 1416 are the vibration of C-H bond in CH_2 and CH_3 and methylene and methyl group having characteristic peaks in the range (2875 cm^{-1} - 2920 cm^{-1}) and (1375 cm^{-1} - 1426 $cm^{-}1$) respectively. The peak at 1639 corresponds to the C=O vibration (1680 cm^{-1}-1480 cm^{-1}). The FTIR peaks at 1073 and 802 is vibration of C-O-H group (1000 cm^{-1}- 1160 cm^{-1}) and wagging of saccharide respectively[66].

Figure3 shows the FTIR absorption spectra for Gel coated Ti substrate. The absorption peak at wavelength 3331 cm^{-1} corresponds to the presence of secondary amine group (3500 cm^{1} - 3310 cm^{-1}) and the peak at 2916 cm^{-1} corresponds to the C-H stretching of alkanes (2962 cm^{-1} to 2853 cm^{-1}). The peak at 1647 cm^{-1} is due to amide C=O stretching which has a characteristic peak in the wavelength range of 1620 cm^{-1} to 1710 cm^{-1}[67]. The N-H bending peak (1650-1500 is shown at 1552 cm^{-1}. N-H out of plane wagging presents at 608 cm^{-1}[67].

FTIR spectrum for SA coated Ti substrate is shown in the Figure4. The broad peak at 3247

cm^{-1} is due to overlapping of C-H and O-H peaks. The sharp peaks at 1405 and 1596 are assigned to the presence of symmetric and asymmetric vibration of carboxylate ions (1460 cm-1- 1649 cm^{-1}). The peaks at 1107 and 935 are due to vibration of C-O pyra-nosyl ring and C-O contribution from C-C-H and C-O-H group respectively[68].

FIGURE 2.

FIGURE 3.

FIGURE 4.

3.2. Open circuit potential (OCP)

OCP indicates the thermodynamic tendency of material during the electrochemical oxidation process. It is an important parameter in order to predict the corrosion behaviour of a material in the absence of induced corrosion effect. The potential varies with time, which is attributed to the changes taking place at the surface of the substrate and stabilizes after a certain period of time. The stabilization nature of potential was observed to be same for all the samples. The potential first shifted to active direction, i.e., becoming more negative, then stabilized eventually.

OCP values of Ti and CS, Gel, and SA coated Ti substrates OCP measurements curves for the Cp-Ti substrate for the different lengths of time, i.e., 1 hour, 3 hours, 6 hours, 12 hours and 24 hours in PBS is shown in the Figure5. The OCP value after 1 hour is observed to be -376.2 mV at zero time which decreases further to a value of -498.4 mV at a time period of 3.6k seconds. In electrolyte. the naturally developed oxide film may grow and dissolve simultaneously[69]. The decrease in the OCP value is associated with the dissolution of the oxide film present on the surface. OCP value after the 3 hours of immersion was -536.3 mV at zero and -542.7 mV at 3.6k seconds respectively. The same trend is observed for the 6 hours, 12 hours and 24 hours immersion time. This indicates relatively shorter period to

achieve thermodynamic equilibrium with an increase in the immersion period. The OCP values decrease further with an increase in immersion time. This decrease in the value is due to increase in corrosion rate with increase in the immersion time period.

The OCP curves for the CS coated Ti are shown in the Figure5. The OCP value for the CS coated Ti is -201.3 mV at zero time period and stabilizes at -258.2 mV for 1 hour immersion time period, which is much lower than the OCP value for the bare Ti substrate (-375.2 mV). This decrease in OCP value indicates the presence of CS layer on the surface. The increase in the immersion time results in increased corrosion rate. The OCP curves for Gel coated Ti are shown in Figure 5. The OCP values for Gel coated substrates were lower than for the Ti substrate but were highest among all biopolymer coated Ti substrates which indicates the least corrosion provided for Gel coated substrate. SA coated Ti substrates exhibit the lowest OCP values, thus the better corrosion protection.

FIGURE 5.

3.3. Electrochemical Impedance Spectroscopy (EIS) Measurements

The EIS results are presented through the Nyquist plot after 24 hours of immersion in PBS solution at ambient temperature. Nyquist plot reflects directly the corrosion resistance of a substrate as diameter of circle indicating the polarization resistance (R_P)[70]. Figure6 presents the Nyquist plot for the uncoated Ti for a time period of 1 hr, 3 hrs, 6 hrs, 12 hrs and 24 hours. Nyquist plot for time period of 1 hour exhibits a inductive loop followed by capacitive loops at higher immersion time period. The presence of inductive loop is attributed to the surface relaxation of species in the oxide layer[71]. The capacitive arc corresponds to the combined effect of double layer and metal dissolution and its diameter is related to charge transfer resistance at metal/electrolyte interface[72]. The Nyquist plots show the depressed semicircles representing the corrosion of Ti which is mainly controlled by charge transfer

process[73]. Critical behaviour was observed for immersion time period of 6 hours, 12 hours and 24 hours, where the substrate resistance increases which may be due to presence of thicker oxide layer. The data were fitted using two different circuit diagrams. Circuit diagram shown in Figure 6(a) was used for fitting the impedance data corresponding to 1 hour immersion in PBS solution. Figure 6(b) was utilised to fit the Nyquist plot for 3 hours, 6 hours 12 hours and 24 hours PBS incubation. The EIS fitted parameters are shown in the Table 1.

FIGURE 6.

TABLE 1.

Figure7 shows the Nyquist plot for CS coated Ti substrates for immersion time period of 1 hour shows a semicircle followed by a straight line. The highest value for the semicircle diameter is observed for the immersion time period of 3 hours showing the highest corrosion resistance. Further increase in the immersion time shows the decreased corrosion resistance value with little deviation for 6 hours, 12 hours and 24 hours. The circuit is shown in Figure 7(a) was used for fitting the date for 1 hour and 6 hours incubation in PBS solution with double capacitive behaviour while Figure 7(b) circuit was used for fitting the data for 3 hours, 12 hours and 24 hours (single capacitive arc). The circuit shown in Figure 7 was used for fitting the data.

FIGURE 7.

TABLE 2.

The Nyquist curve for the Gel coated Ti substrate is shown in Figure 8. The Nyquist curve for the immersion period of 1 hour exhibits the highest arc with an inductive loop which is due to the adsorbed intermediates on the surface[74]. The Nyquist data was utilized for fitting the circuit which is shown in Figure 8 (a). The arc diameter decreases with time, i.e., for 3 hours, 6 hours and 12 hours which is due to increase in corrosion rate with increased immersion time period. The sudden increase in diameter is observed for the time period of 24 hours may be due to thickening of the oxide film. Data were fitted using the circuit shown in Figure 8(b), and fitting parameters shown in Table 3.

FIGURE 8.

TABLE 3.

The Nyquist curve for the SA coated Ti substrate (Figure 9) shows the largest diameter among all the biopolymers which indicates better corrosion resistance. The diameter of the arc first decreases with increased immersion time, i.e., for 1 hour and 3 hours, but then increased with the highest value observed for 24 hours. For all the Nyquist curves, Warburg impedance is seen which shows the resistance to mass transfer indicating the corrosion process under diffusion controlled. The circuit shown in Figure 9 was used for fitting Nyquist data for SA coated Ti substrate and fitting parameters shown in Table 4.

FIGURE 9.

TABLE 4

3.5. ATR-FTIR characterization after incubation in PBS

FTIR spectra after PBS incubation for 24 hours are shown in the Figure10 which shows the presence of adsorbed carbonate (CO_3^{2-}). The vibration at about 1547 cm^{-1}, 1440 cm^{-1}, and

840 cm^{-1} are due to the formation of apatite. The peaks at 1049 cm^{-1}, 1049 cm^{-1}, 1033 cm^{-1} confirms the presence of ionically bonded PO_4^{3-} groups.

PBS incubation of biopolymer coated Titanium substrates significantly alters the FTIR spectra showing the dominant presence of adsorbed carbonate (CO_3^{2-}) related vibration as directly adsorbed (2000-2300 cm^{-1} region) or arising from formed apatite (being approved by bands at about 1547 cm^{-1}, 1440 cm^{-1}, and 840 cm^{-1}), being ionically bonded to -PO_4^{3-} groups (bands at about 1049 cm^{-1}, 1049 cm^{-1}, 1033 cm^{-1})[75].

FIGURE 10.

3.6. SEM characterization after PBS incubation

Scanning Electron Microscope characterization was carried out for the coated substrate after 24 hours incubation in PBS solution. Figure 11 (a) and (b) shows the micrographs for Chitosan coated substrate at different magnifications. SEM studies show the presence of cracks and deposition (carbonate and phosphate groups confirmed by FTIR). SEM micrographs of Gelatin coated Titanium substrate are shown in Figure 12. The surface shows the formation of pits and cracks on the substrate surface. Sodium Alginate coated Titanium substrate shows fewer pits compared to Gelatin coated substrate (Figure 13).

Figure 11

Figure 12

Figure 13

4. Artificial Neural Network prediction for OCP values and Nyquist plots

4.1. Artificial Neural Network Modelling for Prediction of OCP values

The input parameters and NN predicted OCP values are shown in Table 5. The use of NN exhibits excellent accuracy in predicting the OCP values outputs. The input dataset consists of substrate condition normalized values and Time period normalized values. While the normalized OCP values are the target dataset and predicted OCP values is ANN output

dataset. A network with three layers, two neurons for input layer, 10 neurons for hidden layer and one neuron for output layer was designed. The input variables for establishing NN were sample condition and the immersion time. The BPLM trained network was then used to compare the predicted and measured values. Figure 14 represents the comparison between the experimental and predicted OCP values. The R values for training dataset, validation dataset, and test dataset are 0.99999, 1 and 0.99972 respectively, yielding an overall R-value of 0.99813. This clearly indicates the accuracy of ANN in predicting OCP values. The developed model can be used to simulate and predict the OCP values.

FIGURE 14.

4.2. Artificial Neural Network for Prediction of Nyquist plots

The input dataset was randomly divided into training and testing dataset. Back Propagation Bayesian algorithm was used for training and fitting the model. Figures 15, 16, 17 and 18 represents the Nyquist plot for base cp-Titanium, Chitosan coated Titanium, Gelatin coated Titanium and Alginate coated Titanium at different immersion periods respectively. The three-layer network with two neurons for input, twenty neurons for hidden layer and one neuron for output was used. Immersion time period and real part of frequency were the input dataset with the imaginary part of frequency as target dataset. During ANN training the output of the network was measured against the target values. The regression coefficient of R=0.98772 was achieved for bare Titanium substrate (Figure 15(f)). The regression coefficient for Chitosan coated Ti substrate was 0.98821 as shown in Figure 16(f). The Gelatin coated Titanium substrate shows a regression value of 0.94083 (Figure 17(f)). Figure 18(f) shows the regression value of Alginate coated Titanium substrate which is 0.99994. All these regression values indicate the high precision for corrosion modeling and prediction of Nyquist plots.

FIGURE 15.

FIGURE 16.

FIGURE 17.

FIGURE 18

Conclusions

Commercially pure (CP) Titanium substrate was coated with Chitosan, Gelatin B, and Sodium Alginate biopolymers via spin coating technique and corrosion behaviour of the uncoated and coated substrate were studied. All coated cp-Ti substrates showed better corrosion behaviour compared to the uncoated cp-Ti substrate. Sodium Alginate coated Ti substrates shows the highest corrosion resistance among all three biopolymers followed by Gelatin and Chitosan coated cp-Ti substrates. An artificial neural network was developed to model and predict the OCP values for the bare and biopolymer coated Titanium substrates. The values predicted by the present model are in good agreement with the obtained experimental values. Similarly, ANN was also trained in order to predict the Nyquist plot. Therefore, the present ANN model can be used to predict accurately the OCP values for the uncoated and coated substrates.

References

[1] M. Niinomi, M. Nakai, J. Hieda, Development of new metallic alloys for biomedical applications, Acta Biomater. 8 (2012) 3888–3903. doi:10.1016/j.actbio.2012.06.037.

[2] M. Niinomi, Recent metallic materials for biomedical applications, Metall. Mater. Trans. A. 33 (2002) 477–486. doi:10.1007/s11661-002-0109-2.

[3] T.H. Reddy, S. Pal, K.C. Kumar, M.K. Mohan, V. Kokol, Finite element analysis for mechanical response of magnesium foams with regular structure obtained by powder metallurgy method, Procedia Eng. 149 (2016) 425–430. doi:10.1016/j.proeng.2016.06.688.

[4] F.E.T. Heakal, O.S. Shehata, N.S. Tantawy, Integrity of metallic medical implants in physiological solutions, Int. J. Electrochem. Sci. 9 (2014) 1986–2004.

[5] M. Balazic, J. Kopac, M.J. Jackson, W. Ahmed, Review : titanium and titanium alloy applications in medicine, 2007. doi:10.1504/IJNBM.2007.016517.

[6] M. Geetha, A.K. Singh, R. Asokamani, A.K. Gogia, Ti based biomaterials, the ultimate choice for orthopaedic implants - A review, Prog. Mater. Sci. 54 (2009) 397–425. doi:10.1016/j.pmatsci.2008.06.004.

[7] I. Gotman, Characteristics of metals used in implants., J. Endourol. 11 (1997) 383–9. doi:10.1089/end.1997.11.383.

[8] M. Niinomi, Mechanical biocompatibilities of titanium alloys for biomedical applications, J. Mech. Behav. Biomed. Mater. 1 (2008) 30–42. doi:10.1016/j.jmbbm.2007.07.001.

[9] P. Schmutz, N.-C. Quach-Vu, I. Gerber, Metallic medical implants: electrochemical characterization of corrosion processes, Electrochem. Soc. Interface. 17 (2008) 35.

[10] X. Liu, P.K. Chu, C. Ding, Surface modification of titanium, titanium alloys, and related materials for biomedical applications, Mater. Sci. Eng. R Reports. 47 (2004)

49–121. doi:10.1016/j.mser.2004.11.001.

[11] F. Guillemot, Recent advances in the design of titanium alloys for orthopedic applications, Expert Rev. Med. Devices. 2 (2005) 741–748. doi:10.1586/17434440.2.6.741.

[12] C. Veiga, J.P. Davim, PROPERTIES AND APPLICATIONS OF TITANIUM ALLOYS : A BRIEF REVIEW, 32 (2012).

[13] P. Tengvall, I. Lundström, Physico-chemical considerations of titanium as a biomaterial, Clin. Mater. 9 (1992) 115–134. doi:10.1016/0267-6605(92)90056-Y.

[14] M.A. Khan, R.L. Williams, D.F. Williams, In-vitro corrosion and wear of titanium alloys in the biological environment, Biomaterials. 17 (1996) 2117–2126. doi:10.1016/0142-9612(96)00029-4.

[15] S. Tamilselvi, R. Murugaraj, N. Rajendran, Electrochemical impedance spectroscopic studies of titanium and its alloys in saline medium, Mater. Corros. 58 (2007) 113–120. doi:10.1002/maco.200603979.

[16] Osseointegration of titanium , titanium alloy and zirconia dental implants : current knowledge and open questions, 73 (2017) 22–40. doi:10.1111/prd.12179.

[17] J.D. Bumgardner, B.M. Chesnutt, Y. Yuan, Y. Yang, M. Appleford, S. Oh, R. McLaughlin, S.H. Elder, J.L. Ong, The integration of chitosan-coated titanium in bone: an in vivo study in rabbits., Implant Dent. 16 (2007) 66–79. doi:10.1097/ID.0b013e3180312011.

[18] A. Balamurugan, S. Rajeswari, G. Balossier, A.H.S. Rebelo, J.M.F. Ferreira, Corrosion aspects of metallic implants - An overview, Mater. Corros. 59 (2008) 855–869. doi:10.1002/maco.200804173.

[19] H.R. Tiyyagura, B. Munirathinam, B.R. Sunil, L. Neelakantan, R. Willumeit-, M.K. Mohan, V. Kokol, Electrochemical Corrosion Behaviour of Binary Magnesium A

Alloys lloys, 5 (2017) 561–564.

[20] H. Reddy Tiyyagura, K. Chaitanya Kumar, Investigation on Electro-Chemical Behaviour of H 2 SO 4 and HCl Solutions, 5 (2017) 496–499.

[21] M.H.O. Könönen, E.T. Lavonius, J.K. Kivilahti, SEM observations on stress corrosion cracking of commercially pure titanium in a topical fluoride solution, Dent. Mater. 11 (1995) 269–272. doi:10.1016/0109-5641(95)80061-1.

[22] T.E.L. Douglas, S. Kumari, K. Dziadek, M. Dziadek, A. Abalymov, P. Cools, G. Brackman, T. Coenye, R. Morent, M.K. Mohan, A.G. Skirtach, Titanium surface functionalization with coatings of chitosan and polyphenol-rich plant extracts, Mater. Lett. 196 (2017) 213–216. doi:https://doi.org/10.1016/j.matlet.2017.03.065.

[23] A. Di Martino, M. Sittinger, M. V. Risbud, Chitosan: A versatile biopolymer for orthopaedic tissue-engineering, Biomaterials. 26 (2005) 5983–5990. doi:10.1016/j.biomaterials.2005.03.016.

[24] M.I. Sabir, X. Xu, L. Li, A review on biodegradable polymeric materials for bone tissue engineering applications, J. Mater. Sci. 44 (2009) 5713–5724. doi:10.1007/s10853-009-3770-7.

[25] J.D. Bumgardner, R. Wiser, S.H. Elder, R. Jouett, Y. Yang, J.L. Ong, Contact angle, protein adsorption and osteoblast precursor cell attachment to chitosan coatings bonded to titanium., J. Biomater. Sci. Polym. Ed. 14 (2003) 1401–1409. doi:10.1163/156856203322599734.

[26] Z. Wang, X. Zhang, J. Gu, H. Yang, J. Nie, G. Ma, Electrodeposition of alginate/chitosan layer-by-layer composite coatings on titanium substrates, Carbohydr. Polym. 103 (2014) 38–45. doi:10.1016/j.carbpol.2013.12.007.

[27] H. Reddy Tiyyagura, R. Rudolf, S. Gorgieva, R. Fuchs-Godec, V.R. Boyapati, K.M. Mantravadi, V. Kokol, The chitosan coating and processing effect on the physiological

corrosion behaviour of porous magnesium monoliths, Prog. Org. Coatings. 99 (2016) 147–156. doi:10.1016/j.porgcoat.2016.05.019.

[28] P.R. Klokkevold, L. Vandemark, E.B. Kenney, G.W. Bernard, Osteogenesis enhanced by chitosan (poly-N-acetyl glucosaminoglycan) in vitro., J. Periodontol. 67 (1996) 1170–5. doi:10.1902/jop.1996.67.11.1170.

[29] A.R. Costa-Pinto, R.L. Reis, N.M. Neves, Scaffolds Based Bone Tissue Engineering: The Role of Chitosan, Tissue Eng. Part B Rev. 17 (2011) 331–347. doi:10.1089/ten.teb.2010.0704.

[30] M. Rodríguez-vázquez, B. Vega-ruiz, R. Ramos-zúñiga, D.A. Saldaña-koppel, L.F. Quiñones-olvera, Chitosan and Its Potential Use as a Scaffold for Tissue Engineering in Regenerative Medicine, 2015 (2015).

[31] S. Levengood, M. Zhang, Chitosan-based scaffolds for bone tissue engineering, J. Mater. Chem. B. 2 (2014) 3161–3184. doi:10.1039/C4TB00027G.

[32] N. Bhattarai, J. Gunn, M. Zhang, Chitosan-based hydrogels for controlled, localized drug delivery, Adv. Drug Deliv. Rev. 62 (2010) 83–99. doi:10.1016/j.addr.2009.07.019.

[33] Q. Li, D. Yang, G. Ma, Q. Xu, X. Chen, F. Lu, J. Nie, Synthesis and characterization of chitosan-based hydrogels, Int. J. Biol. Macromol. 44 (2009) 121–127. doi:10.1016/j.ijbiomac.2008.11.001.

[34] S. Van Vlierberghe, P. Dubruel, E. Schacht, Biopolymer-based hydrogels as scaffolds for tissue engineering applications: A review, Biomacromolecules. 12 (2011) 1387–1408. doi:10.1021/bm200083n.

[35] M. Szklarska, G. Dercz, W. Simka, K. Dudek, O. Starczewska, M. Łężniak, B. Łosiewicz, Alginate Biopolymer Coatings Obtained by Electrophoretic Deposition on Ti15Mo Alloy, Acta Phys. Pol. A. 125 (2014) 919–923.

doi:10.12693/APhysPolA.125.919.

[36] A. Manuscript, Alginate : properties and biomedical applications, 37 (2013) 106–126. doi:10.1016/j.progpolymsci.2011.06.003.Alginate.

[37] M.G. Carneiro-da-Cunha, M.A. Cerqueira, B.W.S. Souza, S. Carvalho, M.A.C. Quintas, J.A. Teixeira, A.A. Vicente, Physical and thermal properties of a chitosan/alginate nanolayered PET film, Carbohydr. Polym. 82 (2010) 153–159. doi:10.1016/j.carbpol.2010.04.043.

[38] H. Lv, Z. Chen, X. Yang, L. Cen, X. Zhang, P. Gao, Layer-by-layer self-assembly of minocycline-loaded chitosan/alginate multilayer on titanium substrates to inhibit biofilm formation, J. Dent. 42 (2014) 1464–1472. doi:10.1016/j.jdent.2014.06.003.

[39] D.L. Elbert, C.B. Herbert, J.A. Hubbell, Thin polymer layers formed by polyelectrolyte multilayer techniques on biological surfaces, Langmuir. 15 (1999) 5355–5362. doi:10.1021/la9815749.

[40] H.R. Tiyyagura, R. Fuchs-Godec, S. Gorgieva, S. Arthanari, M.K. Mohan, V. Kokol, Biomimetic gelatine coating for less-corrosive and surface bioactive Mg–9Al–1Zn alloys, J. Mater. Res. (2018) 1–14. doi:DOI: 10.1557/jmr.2018.65.

[41] K.B. Djagny, Z. Wang, S. Xu, Gelatin: A Valuable Protein for Food and Pharmaceutical Industries: Review, Crit. Rev. Food Sci. Nutr. 41 (2001) 481–492. doi:10.1080/20014091091904.

[42] K. Cai, A. Rechtenbach, J. Hao, J. Bossert, K.D. Jandt, Polysaccharide-protein surface modification of titanium via a layer-by-layer technique: Characterization and cell behaviour aspects, Biomaterials. 26 (2005) 5960–5971. doi:10.1016/j.biomaterials.2005.03.020.

[43] E.P. Kumar, E.P. Sharma, Artificial Neural Networks-A Study, 2 (2014) 143–148.

[44] P. Mikulskis, A. Hook, A.A. Dundas, D. Irvine, O. Sanni, D. Anderson, R. Langer,

M.R. Alexander, P. Williams, D.A. Winkler, Prediction of Broad-Spectrum Pathogen Attachment to Coating Materials for Biomedical Devices, ACS Appl. Mater. Interfaces. 10 (2018) 139–149. doi:10.1021/acsami.7b14197.

[45] I. Gonzalez-Fernandez, M.A. Iglesias-Otero, M. Esteki, O.A. Moldes, J.C. Mejuto, J. Simal-Gandara, A critical review on the use of artificial neural networks in olive oil production, characterization and authentication, Crit. Rev. Food Sci. Nutr. (2018) 1–14. doi:10.1080/10408398.2018.1433628.

[46] I. Loghmari, Y. Timoumi, A. Messadi, Performance comparison of two global solar radiation models for spatial interpolation purposes, Renew. Sustain. Energy Rev. 82 (2018) 837–844. doi:https://doi.org/10.1016/j.rser.2017.09.092.

[47] H.K. Ghritlahre, R.K. Prasad, Application of ANN technique to predict the performance of solar collector systems - A review, Renew. Sustain. Energy Rev. 84 (2018) 75–88. doi:https://doi.org/10.1016/j.rser.2018.01.001.

[48] Y. Liu, S. Yu, Y. Zhu, D. Wang, J. Liu, Modeling, planning, application and management of energy systems for isolated areas: A review, Renew. Sustain. Energy Rev. 82 (2018) 460–470. doi:https://doi.org/10.1016/j.rser.2017.09.063.

[49] Z. Sabir, M.A. Manzar, M.A.Z. Raja, M. Sheraz, A.M. Wazwaz, Neuro-heuristics for nonlinear singular Thomas-Fermi systems, Appl. Soft Comput. 65 (2018) 152–169. doi:https://doi.org/10.1016/j.asoc.2018.01.009.

[50] Y. Li, S. Hu, X. Sun, M. Stan, A review: Applications of the phase field method in predicting microstructure and property evolution of irradiated nuclear materials, Npj Comput. Mater. 3 (2017). doi:10.1038/s41524-017-0018-y.

[51] G. Hinton, L. Deng, D. Yu, G.E. Dahl, A. Mohamed, N. Jaitly, A. Senior, V. Vanhoucke, P. Nguyen, T.N. Sainath, B. Kingsbury, Deep Neural Networks for Acoustic Modeling in Speech Recognition, IEEE Signal Process. Mag. (2012) 82–97.

doi:10.1109/MSP.2012.2205597.

[52] L. Deng, G. Hinton, B. Kingsbury, New types of deep neural network learning for speech recognition and related applications: an overview, 2013 IEEE Int. Conf. Acoust. Speech Signal Process. (2013) 8599–8603. doi:10.1109/ICASSP.2013.6639344.

[53] N. Lin, F. Xie, J. Zou, H. Wang, B. Tang, Application of artificial neural network in predicting the thickness of chromizing coatings on P110 steel, J. Wuhan Univ. Technol. Mater. Sci. Ed. 28 (2013) 196–201. doi:10.1007/s11595-013-0664-y.

[54] N. Haghdadi, A. Zarei-Hanzaki, A.R. Khalesian, H.R. Abedi, Artificial neural network modeling to predict the hot deformation behavior of an A356 aluminum alloy, Mater. Des. 49 (2013) 386–391. doi:10.1016/j.matdes.2012.12.082.

[55] S. Malinov, W. Sha, Application of artificial neural networks for modelling correlations in titanium alloys, Mater. Sci. Eng. A. 365 (2004) 202–211. doi:10.1016/j.msea.2003.09.029.

[56] A. Saxena, N. Verma, K.C. Tripathi, A Review Study of Weather Forecasting Using Artificial Neural Network Approach, Int. J. Eng. Res. Technol. 2 (2013) 2029–2035.

[57] P.J. Lisboa, A.F.G. Taktak, The use of artificial neural networks in decision support in cancer: A systematic review, Neural Networks. 19 (2006) 408–415. doi:10.1016/j.neunet.2005.10.007.

[58] Z.-H. Zhou, Y. Jiang, Y.-B. Yang, S.-F. Chen, Lung cancer cell identification based on artificial neural network ensembles, Artif. Intell. Med. 24 (2002) 25–36. doi:10.1016/S0933-3657(01)00094-X.

[59] a S. Miller, B.H. Blott, T.K. Hames, Review of neural network applications in medical imaging and signal processing, Med Biol Eng Comput. 30 (1992) 449–64 ST–Review of neural network applications.

[60] M. Kamrunnahar, M. Urquidi-Macdonald, Prediction of corrosion behavior using neural network as a data mining tool, Corros. Sci. 52 (2010) 669–677. doi:10.1016/j.corsci.2009.10.024.

[61] D. Mareci, G.D. Suditu, R. Chelariu, L.C. Trincă, S. Curteanu, Prediction of corrosion resistance of some dental metallic materials applying artificial neural networks, Mater. Corros. (2016) n/a-n/a. doi:10.1002/maco.201608848.

[62] J. Shi, J. Wang, D.D. Macdonald, Prediction of primary water stress corrosion crack growth rates in Alloy 600 using artificial neural networks, Corros. Sci. 92 (2015) 217–227. doi:10.1016/j.corsci.2014.12.007.

[63] F. Mansfeld, Use of electrochemical impedance spectroscopy for the study of corrosion protection by polymer coatings I ---I I, J. Appl. Electrochem. 25 (1995) 187–202. doi:10.1007/BF00262955.

[64] J. Titz, G.H. Wagner, H. Spáhn, M. Ebert, K. Jüttner, W.J. Lorenz, Characterization of Organic Coatings on Metal Substrates by Electrochemical Impedance Spectroscopy, Corrosion. 46 (1990) 221–229. doi:10.5006/1.3585095.

[65] M. Correa, C. Bielza, M.D.J. Ramirez, J.R. Alique, A Bayesian network model for surface roughness prediction in the machining process, Int. J. Syst. Sci. 39 (2008) 1181–1192. doi:10.1080/00207720802344683.

[66] G. Lawrie, I. Keen, B. Drew, A. Chandler-Temple, L. Rintoul, P. Fredericks, L. Gr??ndahl, Interactions between alginate and chitosan biopolymers characterized using FTIR and XPS, Biomacromolecules. 8 (2007) 2533–2541. doi:10.1021/bm070014y.

[67] J.B. Science, T. Nguyen, B. Lee, Fabrication and characterization of cross-linked gelatin, 2010 (2010) 1117–1124. doi:10.4236/jbise.2010.312145.

[68] Z. a Nur Hanani, Y.H. Roos, J.P. Kerry, Fourier Transform Infrared (FTIR) Spectroscopic Analysis of Biodegradable Gelatin Films Immersed in Water, 11th Int.

Congr. Eng. Food. 5 (2011) 6–9.

[69] A.A. Ghoneim, A.S. Mogoda, K.A. Awad, F.E. Heakal, Electrochemical Studies of Titanium and its Ti-6Al-4V Alloy in Phosphoric Acid Solutions, Int. J. Electrchem. Sci. 7 (2012) 6539–6554.

[70] F. Song, C. Wu, H. Chen, Q. Liu, J. Liu, R. Chen, R. Li, J. Wang, Water-repellent and corrosion-resistance properties of superhydrophobic and lubricant-infused super slippery surfaces, RSC Adv. 7 (2017) 44239–44246. doi:10.1039/c7ra04816e.

[71] A. Yurt, S. Ulutas, H. Dal, Electrochemical and theoretical investigation on the corrosion of aluminium in acidic solution containing some Schiff bases, Appl. Surf. Sci. 253 (2006) 919–925. doi:10.1016/j.apsusc.2006.01.026.

[72] S. Benserradj, The Effect of surface treatments on the electrochemical behavior of Titanium alloy in seawater by electrochemical impedance spectroscopy (EIS), 6 (2015) 1829–1833.

[73] Q. Qu, L. Wang, Y. Chen, L. Li, Y. He, Z. Ding, Corrosion behavior of titanium in artificial saliva by lactic acid, Materials (Basel). 7 (2014) 5528–5542. doi:10.3390/ma7085528.

[74] M. Keddam, C. Kuntz, H. Takenouti, D. Schustert, D. Zuili, Exfoliation corrosion of aluminium alloys examined by electrode impedance, Electrochim. Acta. 42 (1997) 87–97. doi:10.1016/0013-4686(96)00170-3.

[75] L. Berzina-Cimdina, N. Borodajenko, Research of Calcium Phosphates Using Fourier Transform Infrared Spectroscopy, Infrared Spectrosc. – Mater. Sci. Eng. Technol. (2012) 123–148. doi:10.5772/36942.

Figures and Tables

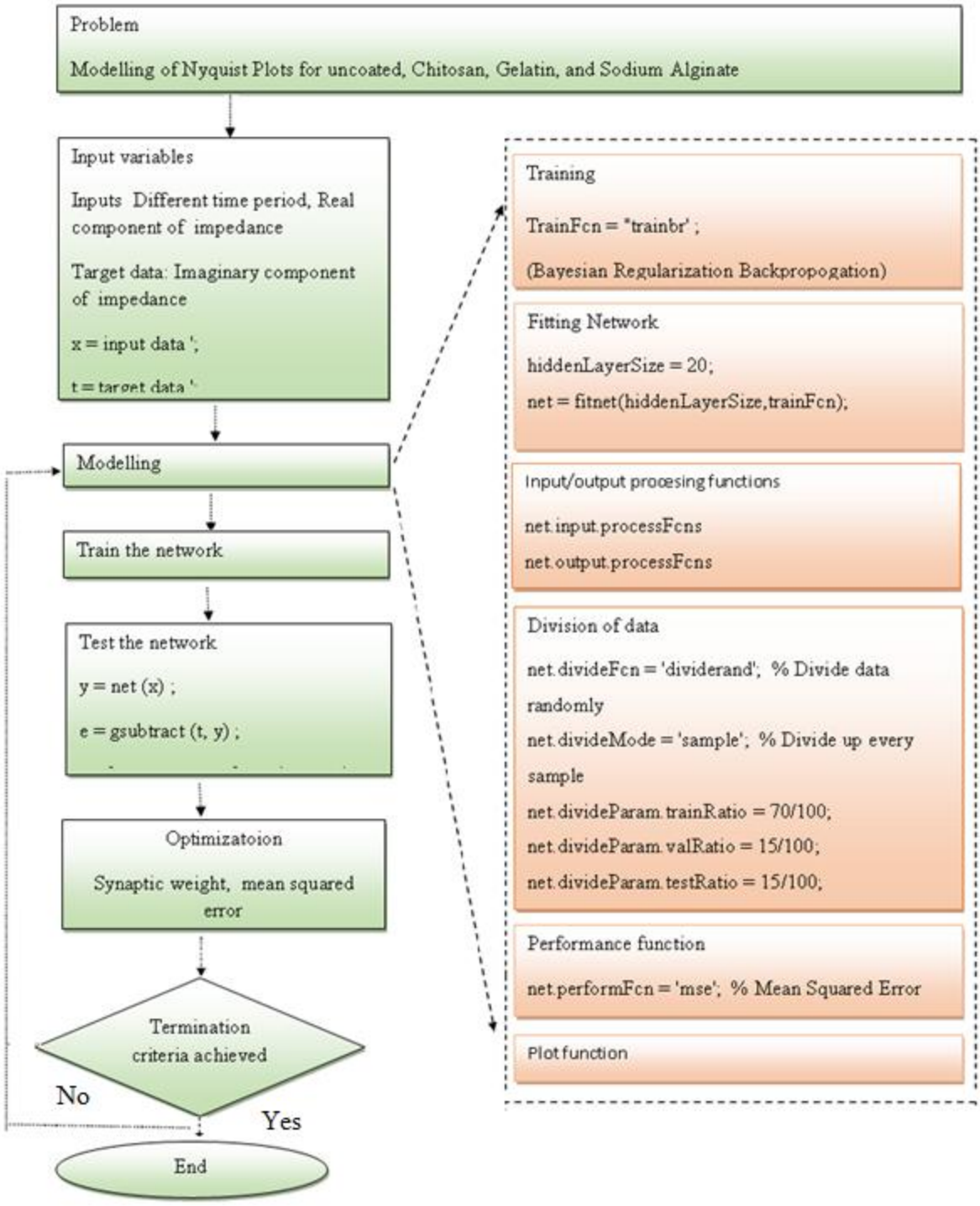

Figure 1. Pseudocode for prediction of Nyquist plot

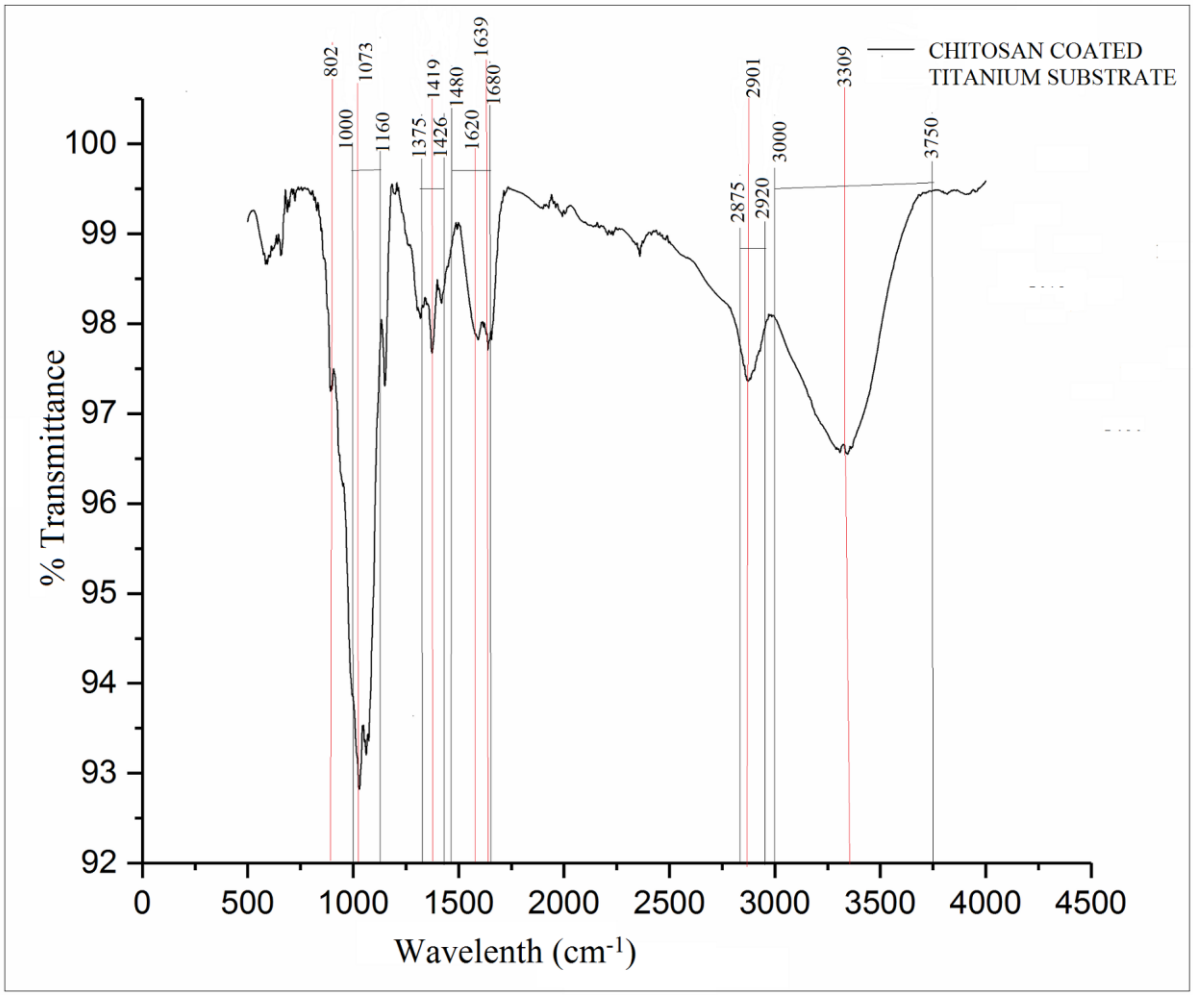

Figure 2. ATR-FTIR curve for Chitosan coated cp-Titanium substrate

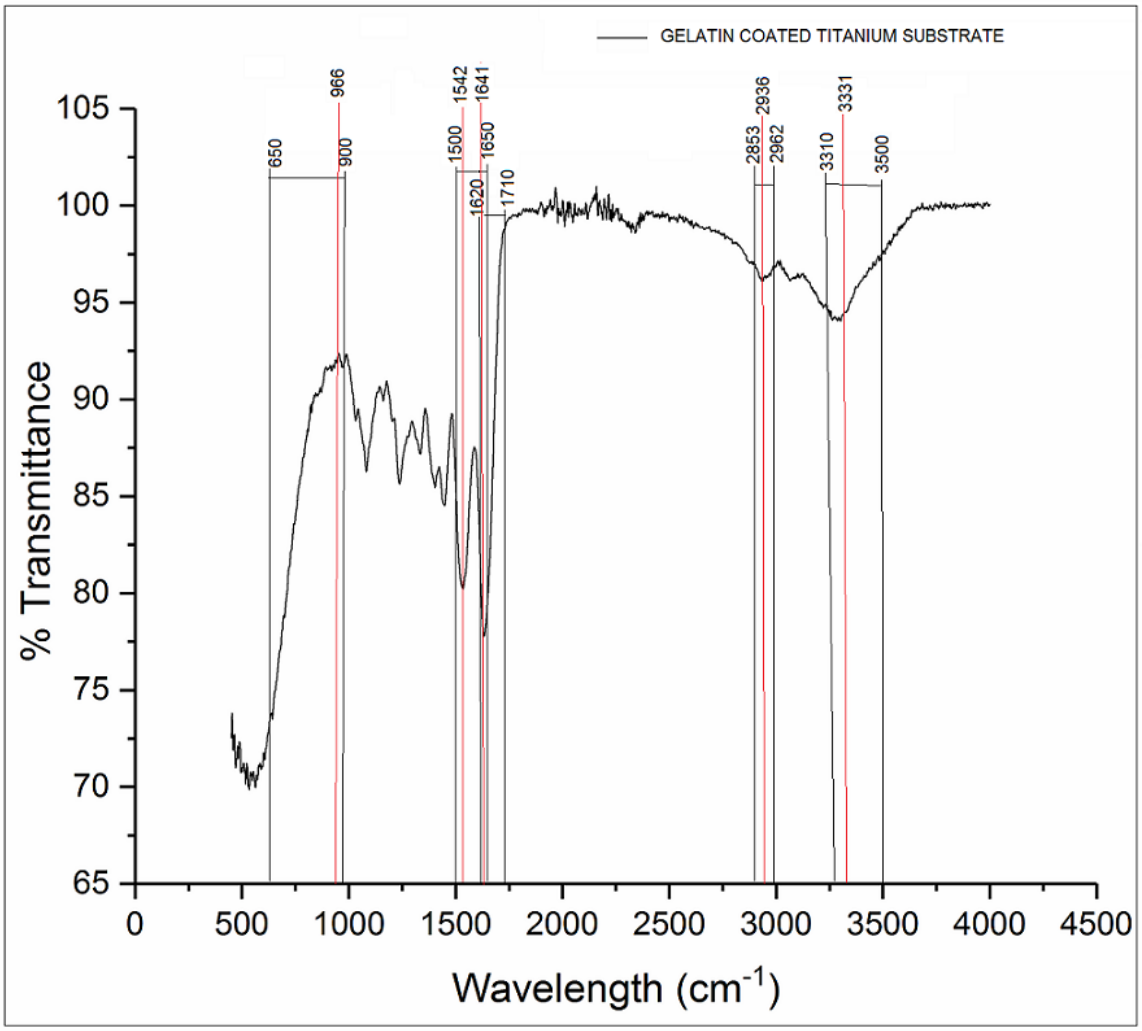

Figure 3. ATR-FTIR curve for Gelatin coated cp-Titanium substrate

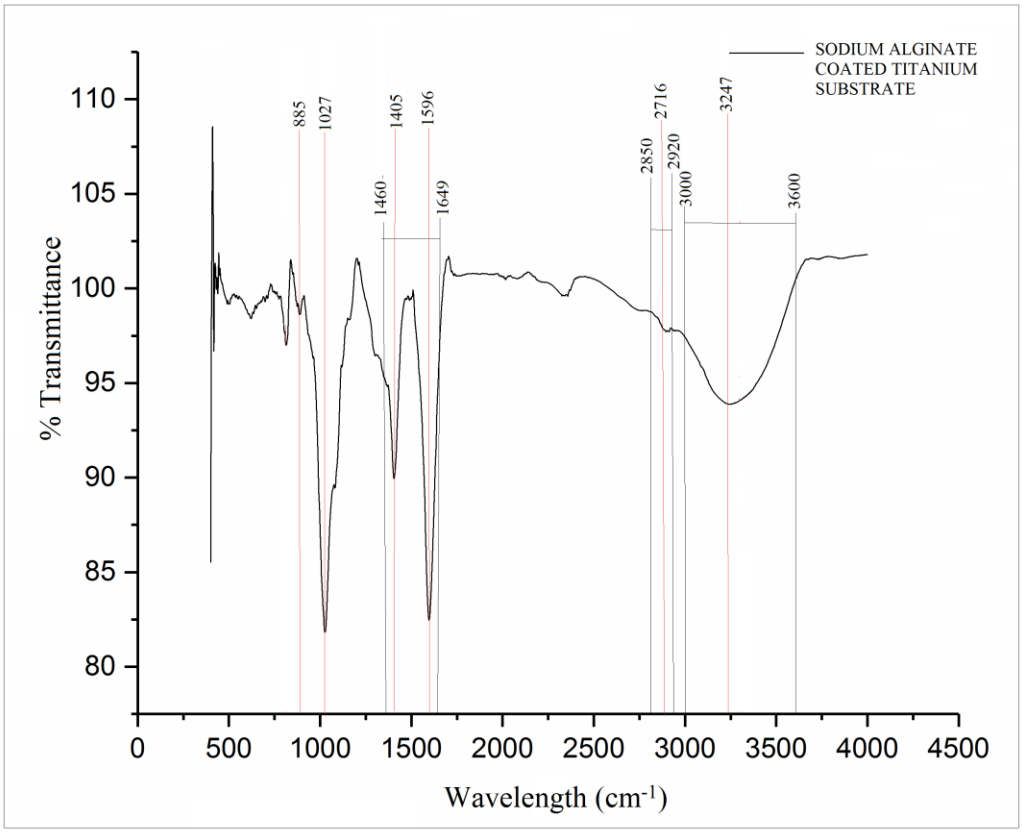

Figure 4. ATR-FTIR curve for Sodium Alginate coated cp-Titanium substrate

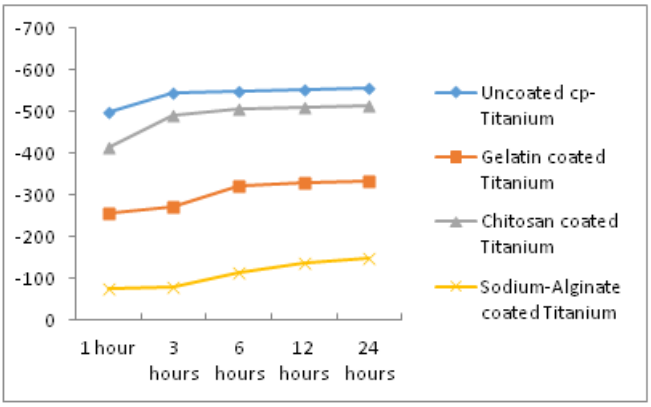

Figure 5. Open Circuit Potential for all uncoated and biopolymer coated Titanium substrate at different time intervals in PBS

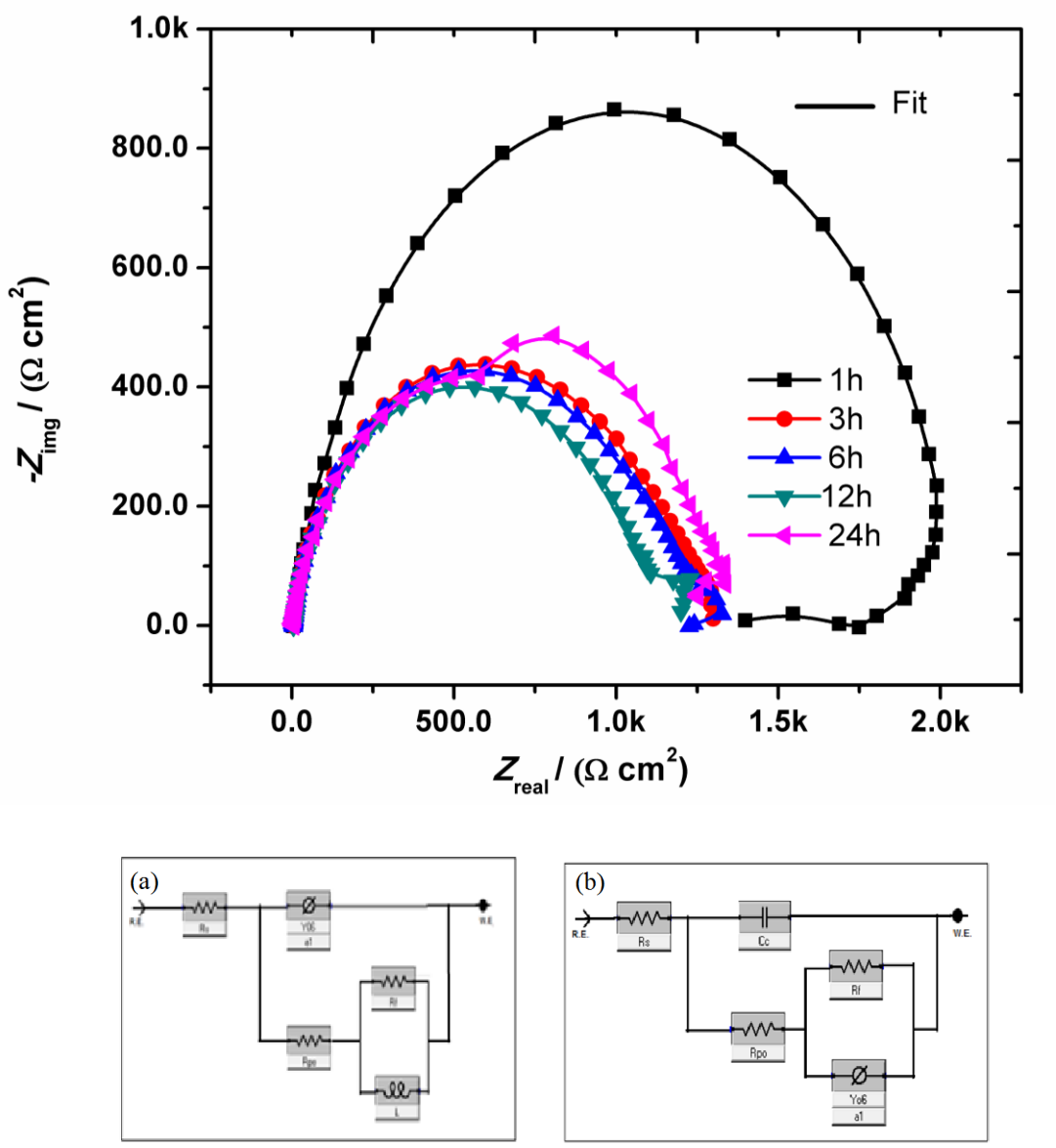

Figure 6. Nyquist plot for uncoated Titanium substrate, (a) circuit used for fitting Nyquist data for 1 hour of PBS immersion, (b) circuit used for fitting Nyquist data for 3 hours, 6 hours, 12 hours and 24 hours of PBS immersion

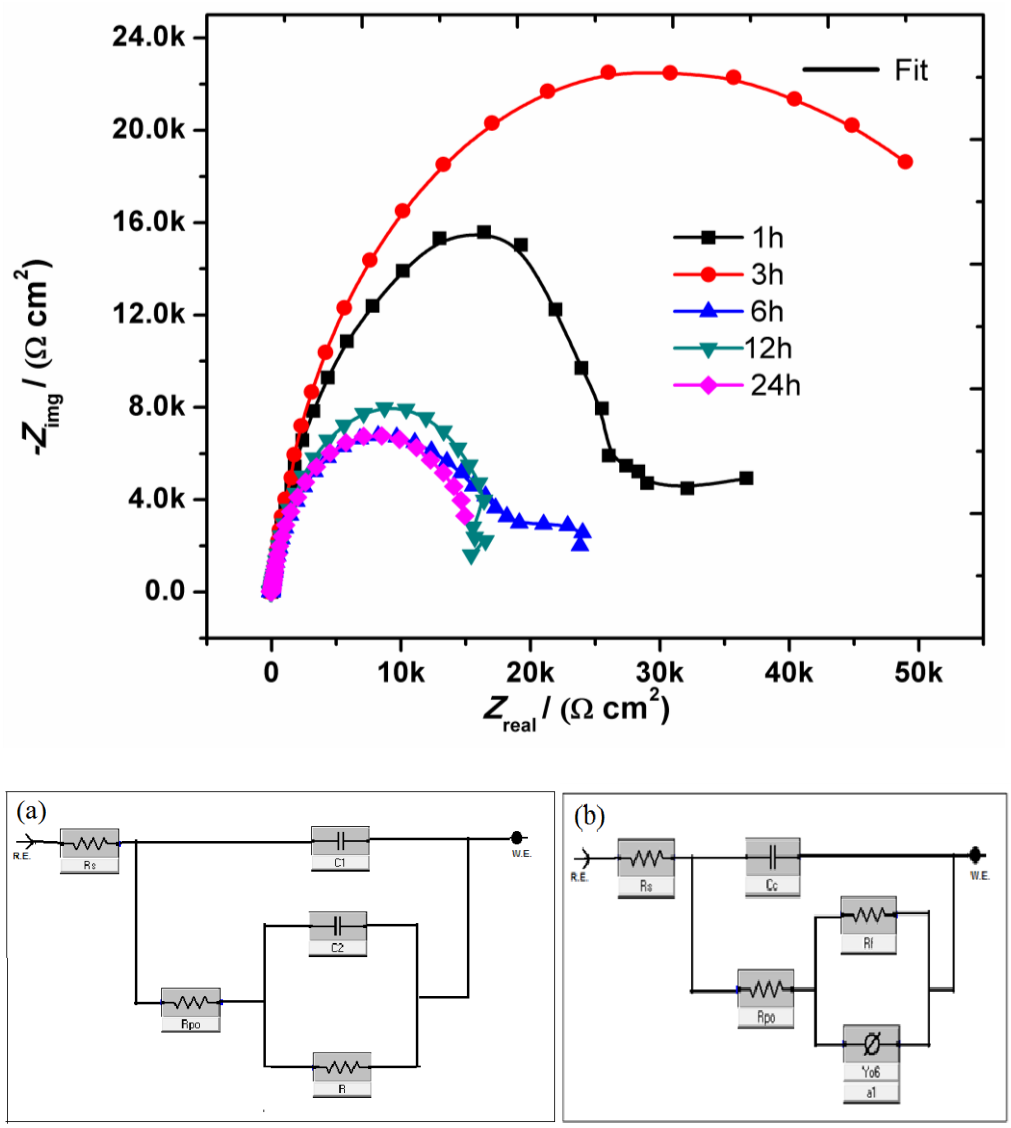

Figure 7. Nyquist plot for Chitosan coated Titanium substrate, (a) circuit used for fitting Nyquist data for 1 hour and 6 hours immersion, (b) circuit used for fitting Nyquist data for 3 hours, 12 hours and 24 hours of PBS immersion

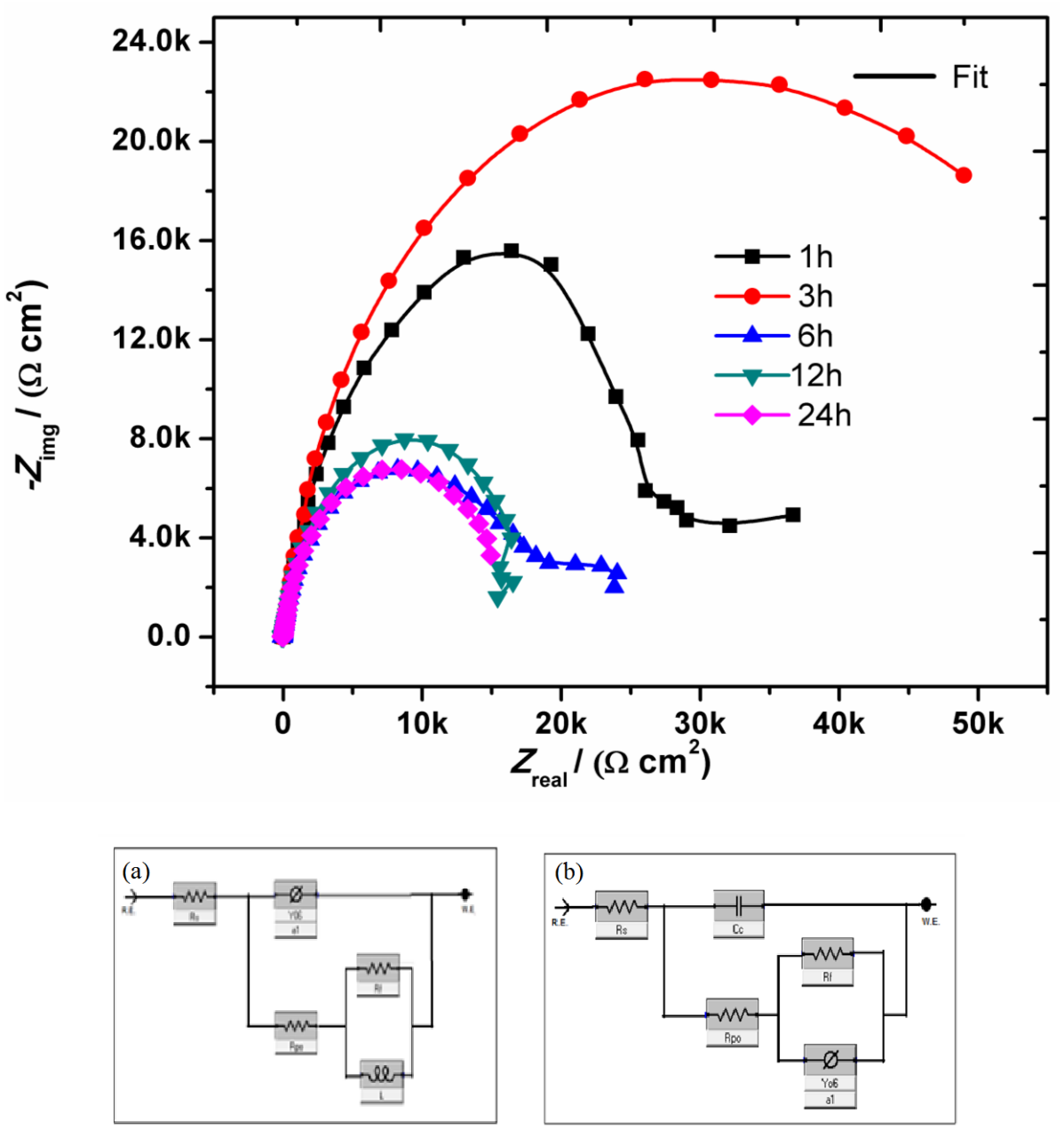

Figure 8. Nyquist plot for Gelatin coated Titanium substrate, (a) circuit used for fitting Nyquist data for 1 hour immersion, (b) circuit used for fitting the data for 3 hours, 6 hours, 12 hours and 24 hours PBS immersion

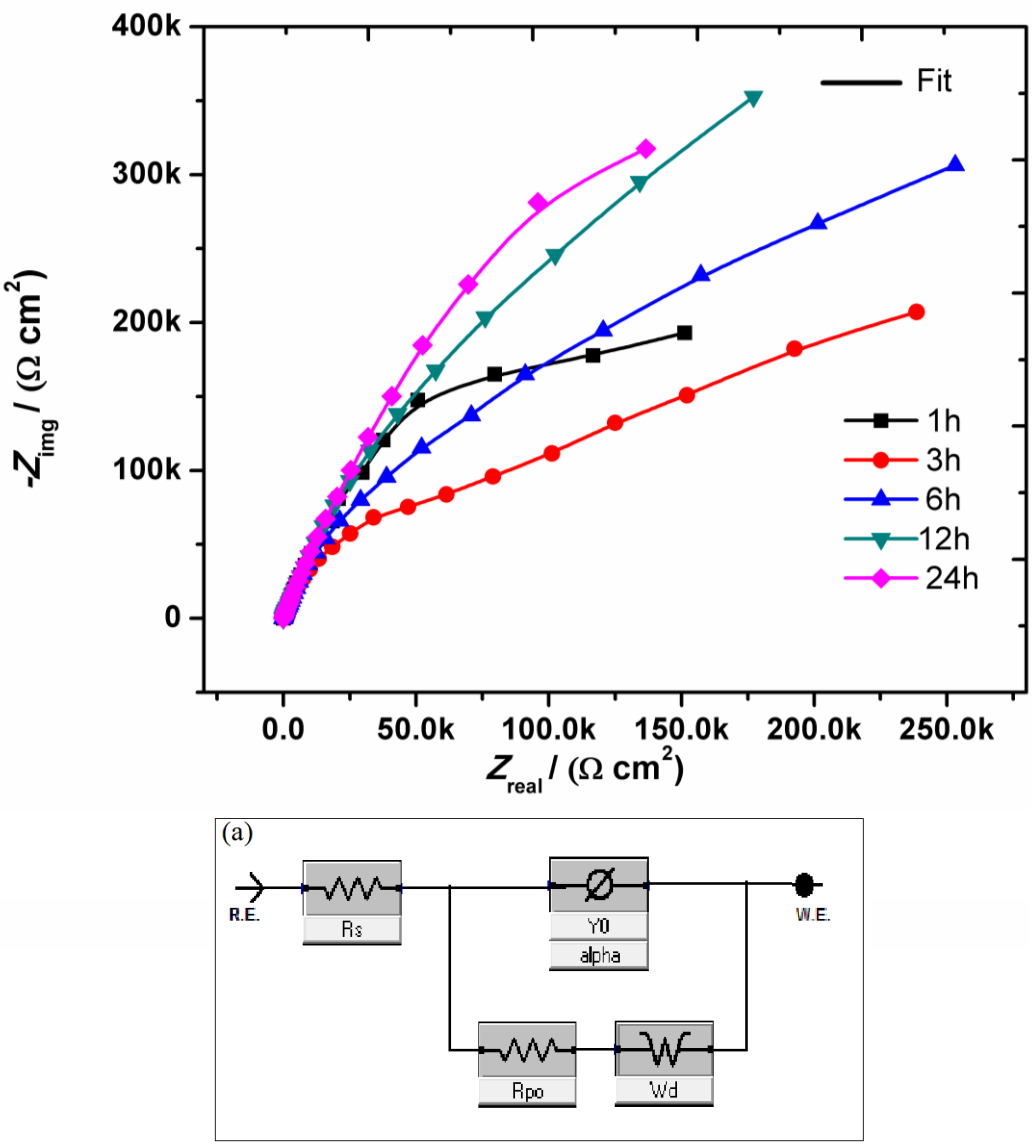

Figure 9. Nyquist plot for Sodium Alginate coated Titanium substrate (a) circuit used for fitting the Nyquist data

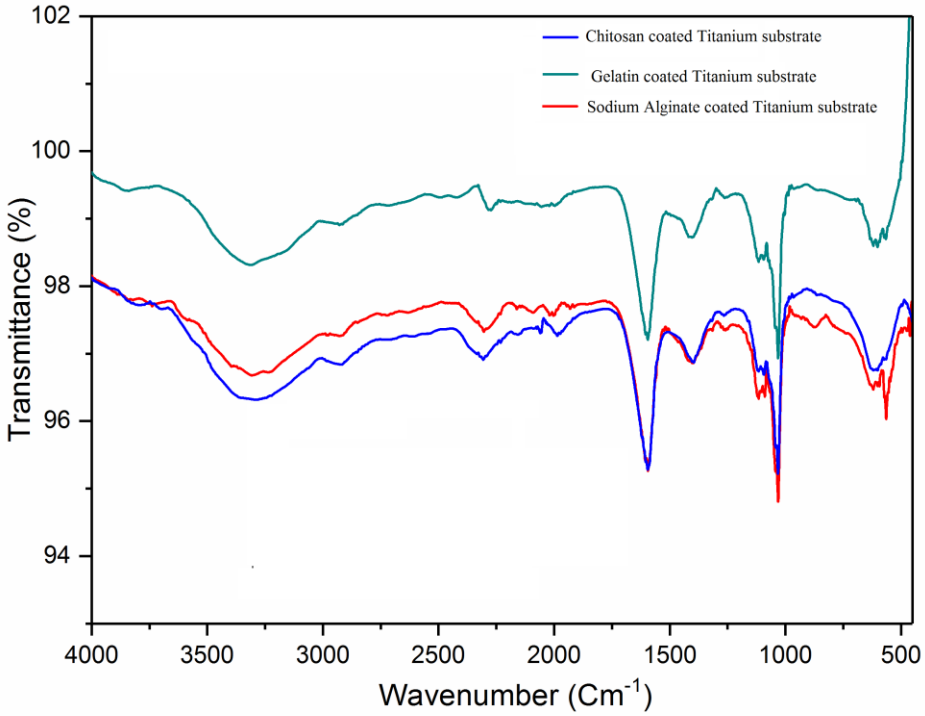

Figure 10. FTIR spectra for biopolymer coated Titanium after PBS incubation for 24 hours

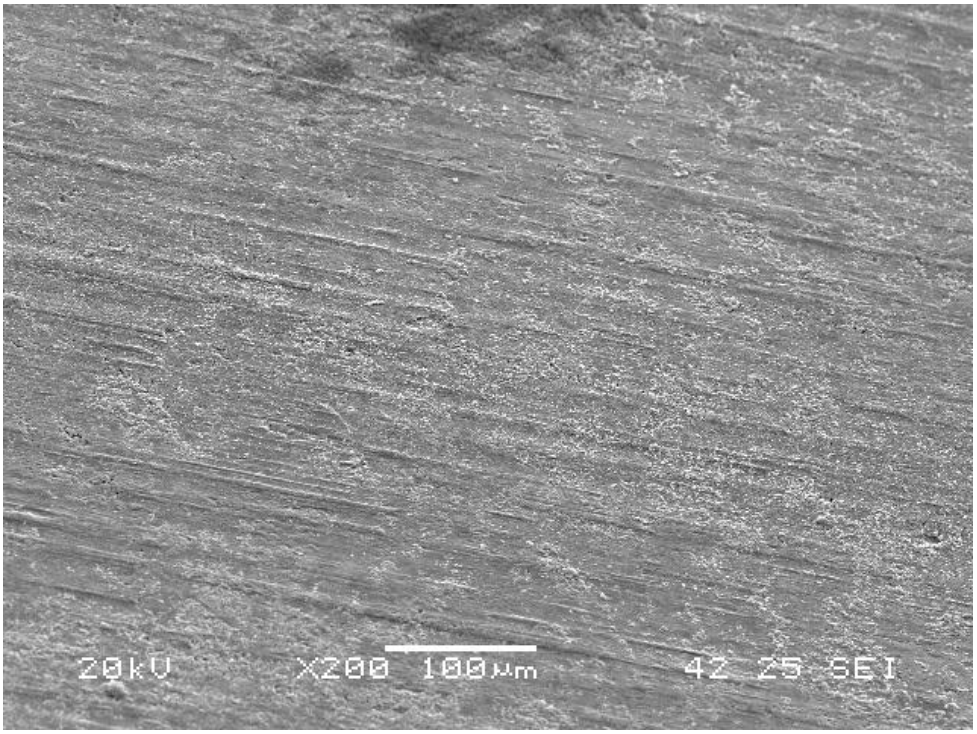

(a)

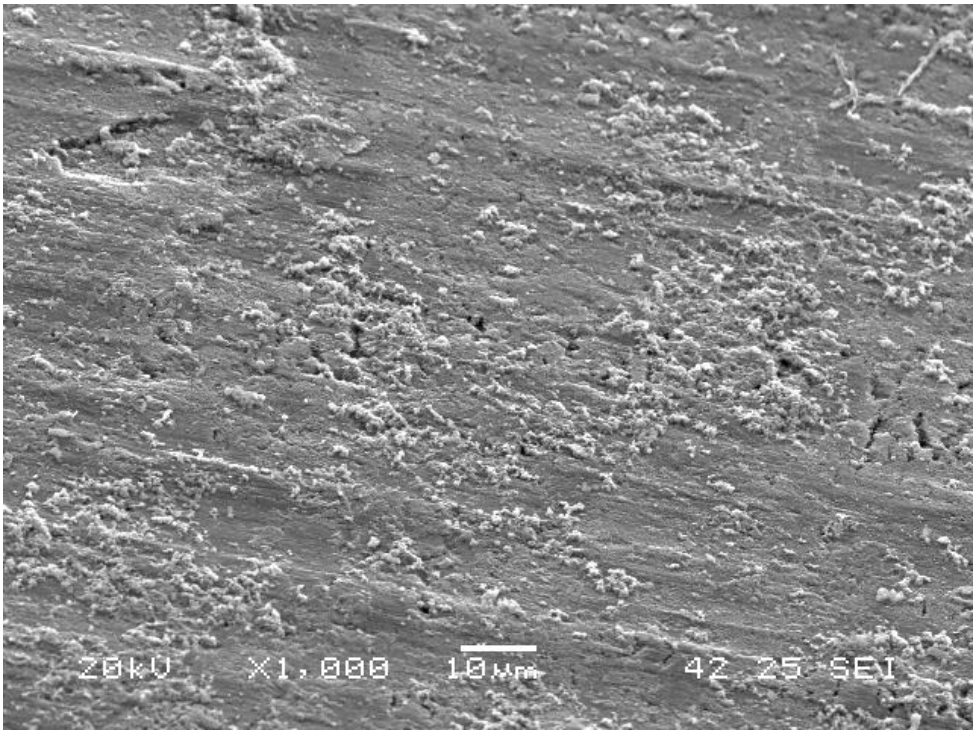

(b)

Figure 11. SEM micrographs for Chitosan coated Titanium after PBS incubation

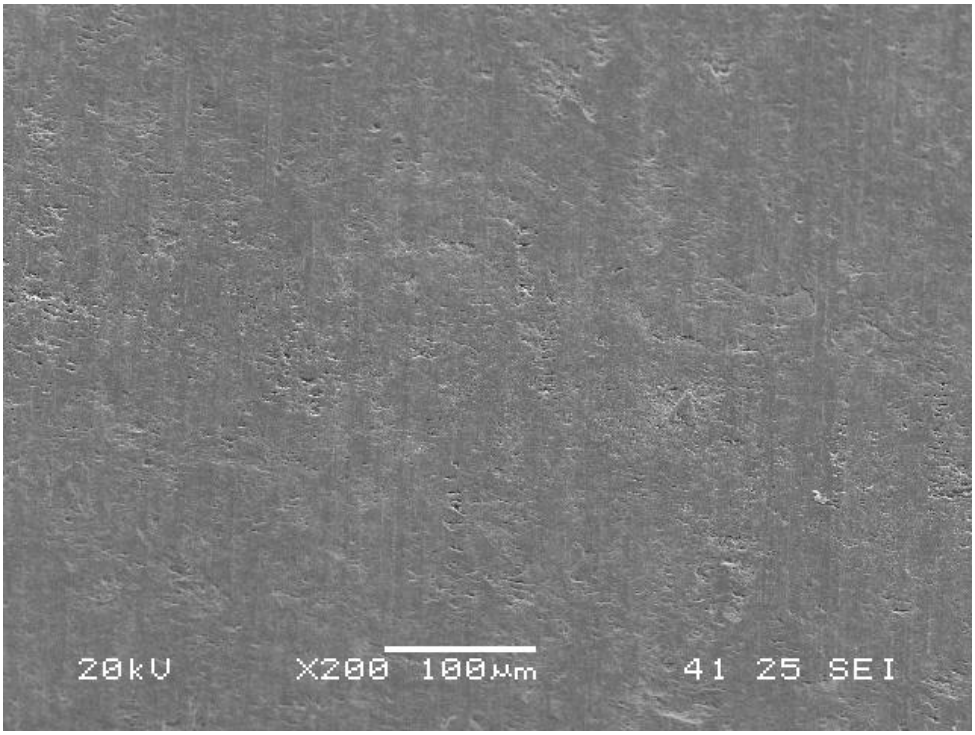

(a)

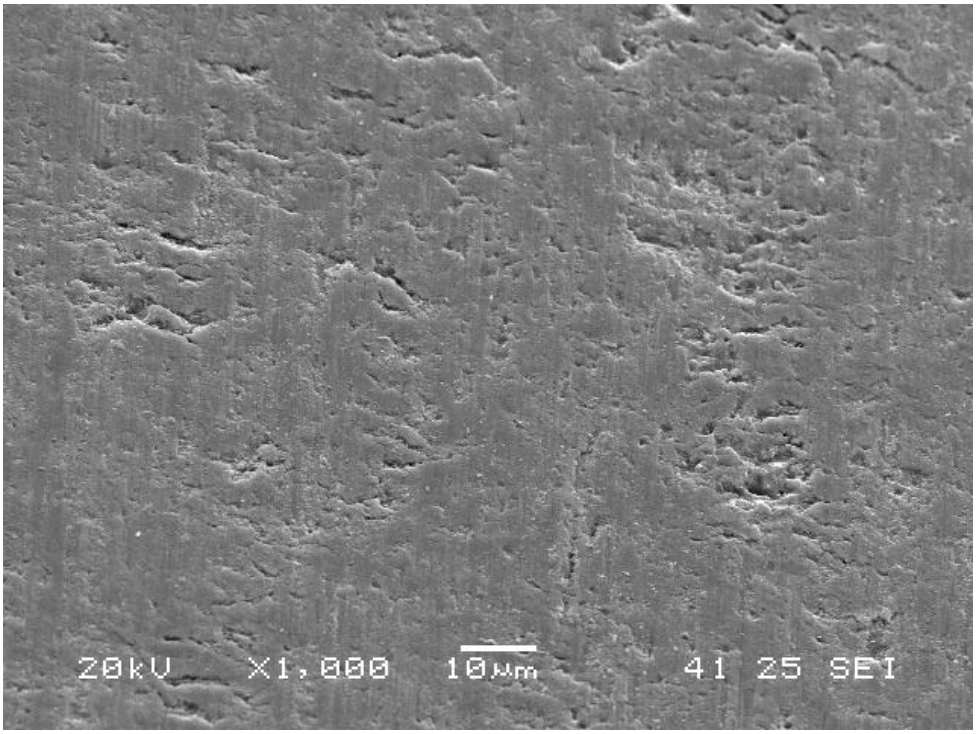

(b)

Figure 12. SEM micrographs for Gelatin coated Titanium after PBS incubation

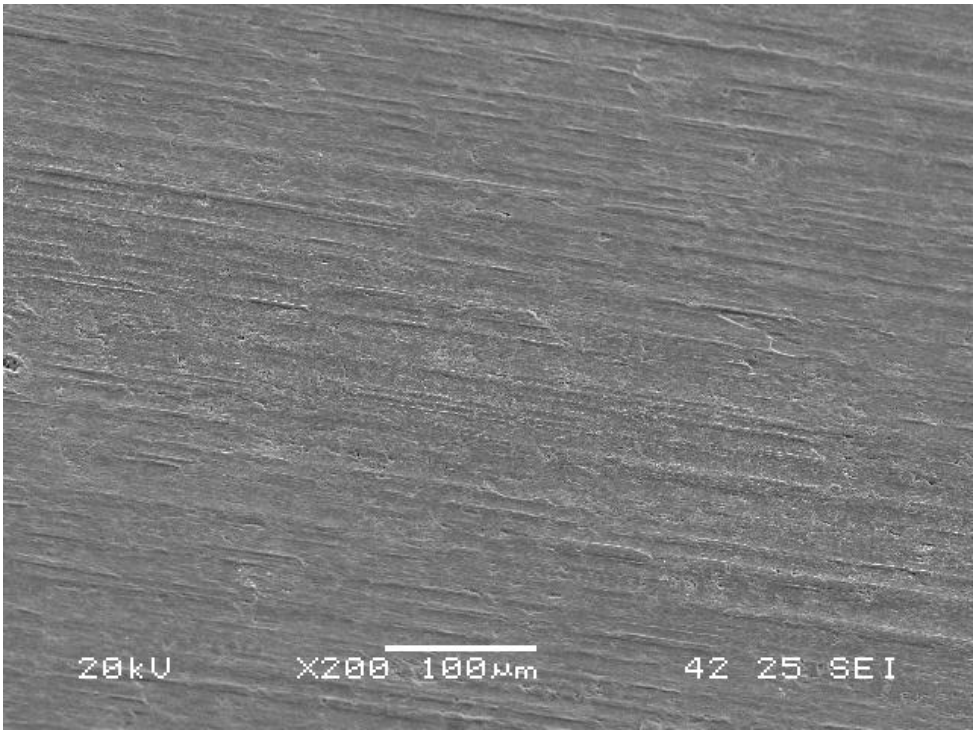

(a)

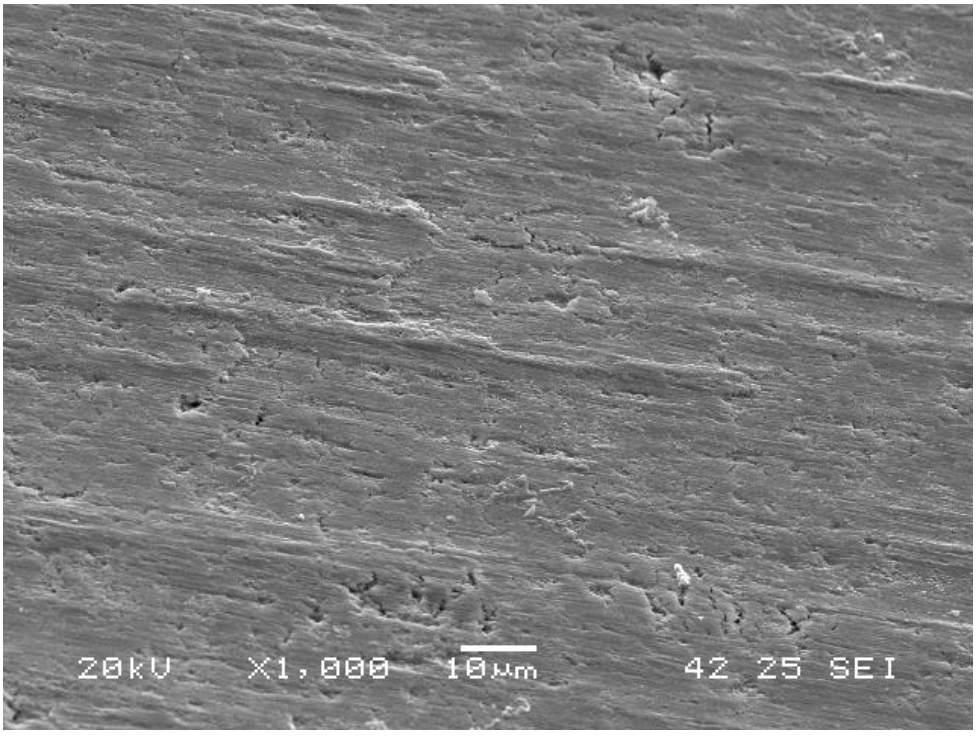

(b)

Figure 13. SEM micrographs for Sodium Alginate coated Titanium after PBS incubation

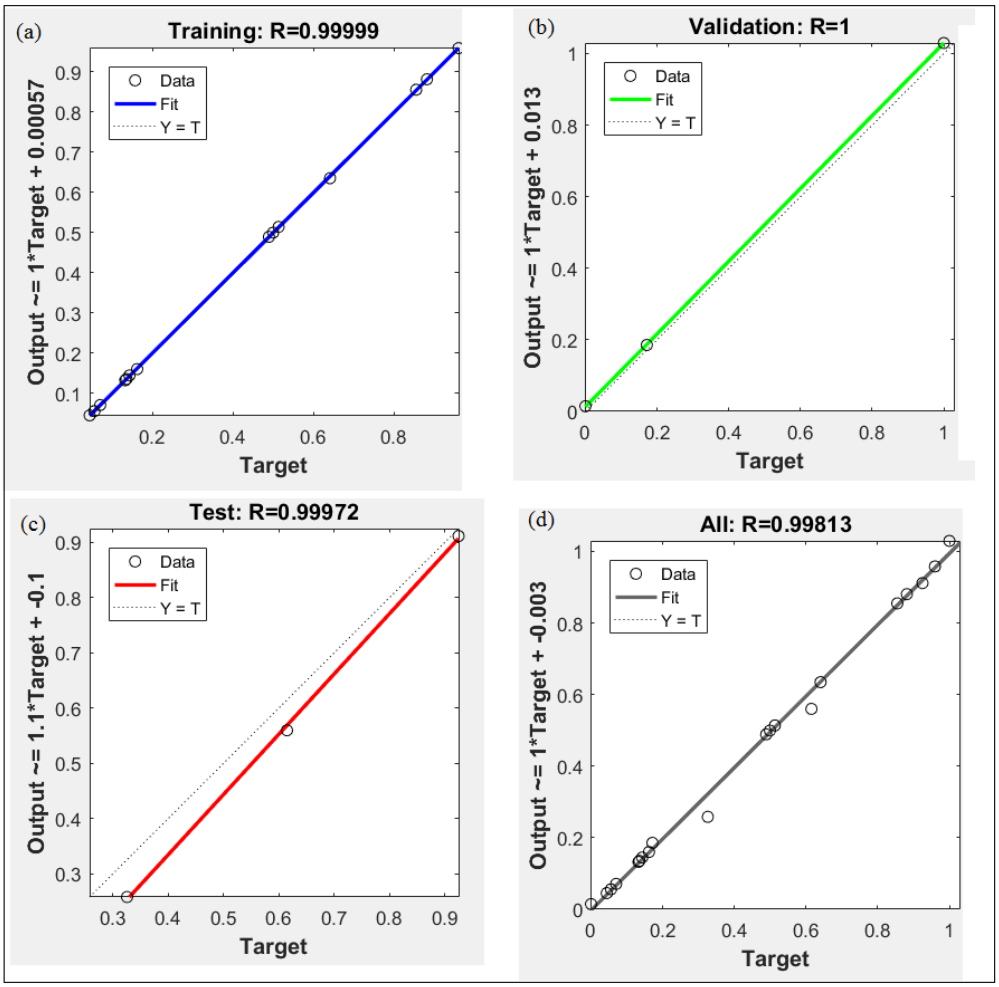

Figure 14. Regression values for the training, validation and test dataset for OCP prediction

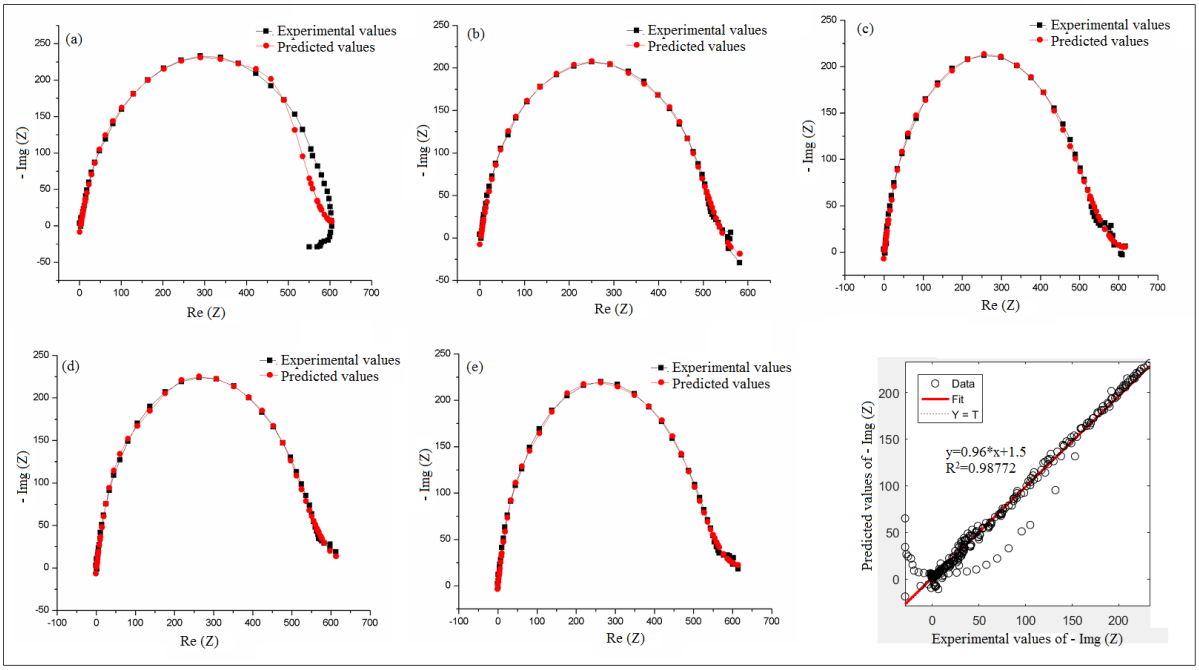

Figure 15. Nyquist plots obtained bare cp-Titanium (experimental and ANN predicted) for immersion periods; (a) 1 hour; (b) 3 hours; (c) 6 hours; (d) 12 hours; (e) 24 hours; (f) Regression values obtained for the network for Nyquist plot of cp-Titanium

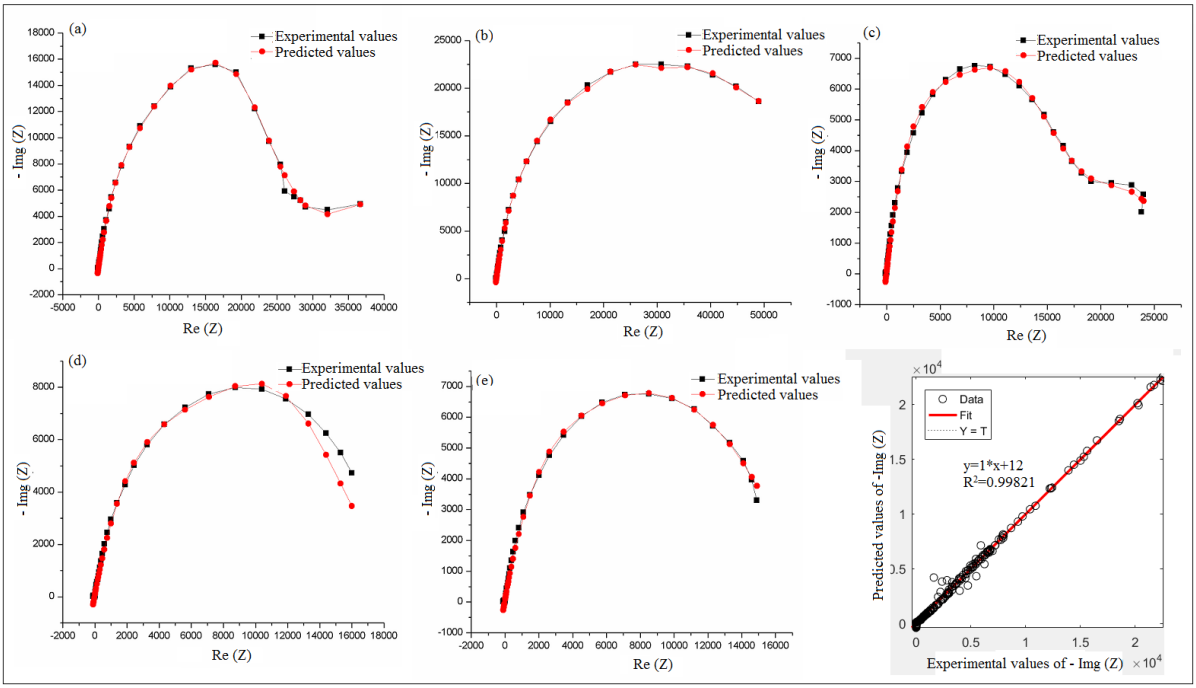

Figure 16. Nyquist plots obtained Chitosan coated cp-Titanium (experimental and ANN predicted) the immersion periods; (a) 1 hour; (b) 3 hours; (c) 6 hours; (d) 12 hours; (e) 24 hours; (f) Regression values obtained for the network for Nyquist plot of Chitosan coated cp-Titanium

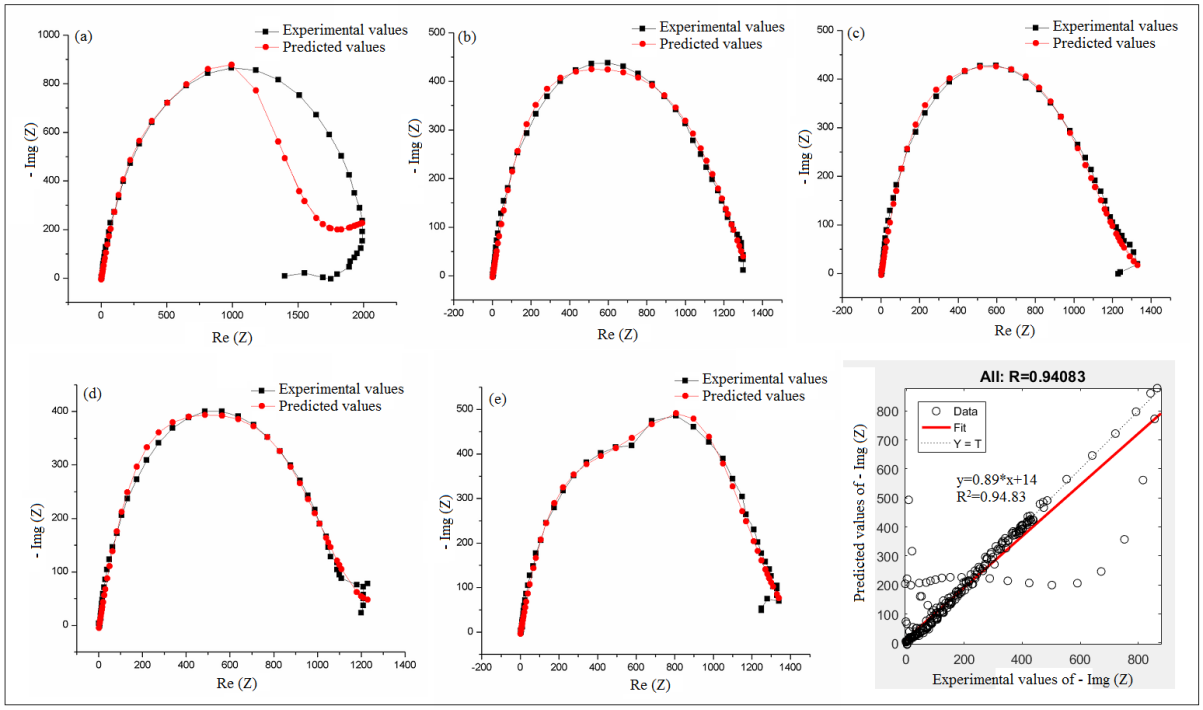

Figure 17. Nyquist plots obtained Gelatin coated cp-Titanium (experimental and ANN predicted) the immersion periods; (a) 1 hour; (b) 3 hours; (c) 6 hours; (d) 12 hours; (e) 24 hours; (f) Regression values obtained for the network for Nyquist plot of Gelatin coated cp-Titanium

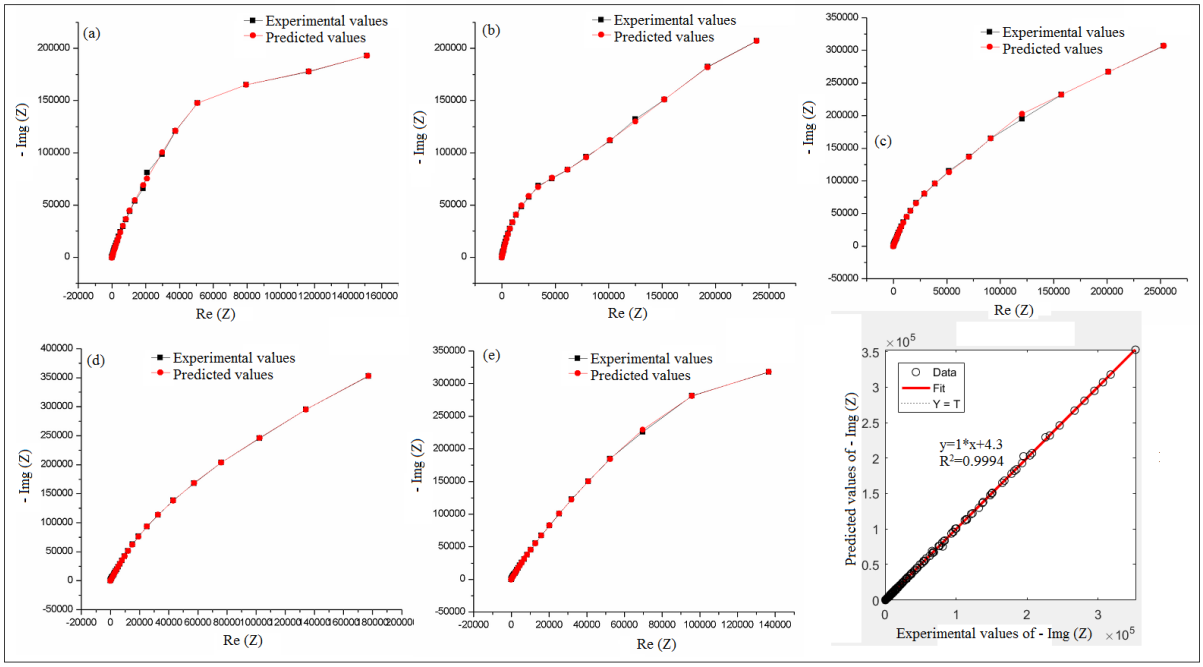

Figure 18. Nyquist plots obtained Alginate coated cp-Titanium (experimental and ANN predicted) the immersion periods; (a) 1 hour; (b) 3 hours; (c) 6 hours; (d) 12 hours; (e) 24 hours; (f) Regression values obtained for the network for Nyquist plot of Alginate coated cp-Titanium

Table 1.EIS fitting parameters of uncoated Ti substrates for Nyquist plot

Time period	R_{po} (Ω)	R_f (Ω)	C_c (F) (e^{-6})	R_u (Ω)	L	Yo6 (e^{-6})	a7 (e^{-3})
1 hour	537.6	70.41	------	2.818	$5.982e^{3}$	695.5	839.3
3 hours	3.795	550.8	181.1	2.876	------	473.6	789.6
6 hours	9.648	550.8	221.2	1.791	------	444.3	766.4
12 hours	21.20	556.0	252.0	$972.2e^{-3}$	------	408.1	741.1
24 hours	505.1	80.83	712.8	$998.2e^{-3}$	------	645.5	897.6

Table 2. EIS fitting parameters of Chitosan coated Ti substrates for Nyquist plot

Time Period	R_{po} (Ω)	C_c (F)	R_f (Ω)	R_u (Ω)	Yo6	a7 (e^{-3})
1 hour	5.097	$71.28e^{-6}$	$33.18e^{3}$	3.106	$225.4e^{-6}$	831.5
3 hours	3.534	$447.8e^{-9}$	$57.23e^{3}$	$11.57e^{-6}$	$280.3e^{-6}$	876.0
6 hours	3.566	$420.7e^{-9}$	$19.72e^{3}$	$24.10e^{-6}$	$318.5e^{-6}$	856.4
12 hours	3.660	$522.9e^{-9}$	$18.13e^{3}$	$18.43e^{-6}$	$291.6e^{-6}$	868.2
24 hours	3.672	$459.8e^{-9}$	$17.01e^{3}$	$39.97e^{-6}$	$303.2e^{-6}$	860.7

Table 3. EIS fitting parameters of Gelatin coated substrates for Nyquist plot

Time Period	R_{po} (Ω)	C_c (F)	R_f (Ω)	R_u (Ω)	L	Yo6	a7
1 hour	$1.696e^{3}$	------	397.0	4.338	$11.69e^{3}$	$559.1e^{-6}$	$860.7e^{-3}$
3 hours	$1.007e^{3}$	$356.2e^{-6}$	160.7	4.611	------	$66.03e^{-3}$	$853.7e^{-3}$
6 hours	3.408	$102.7e^{-6}$	$1.199e^{3}$	4.327	------	$486.0e^{-6}$	$807.6e^{-3}$
12 hours	3.021	$99.36e^{-6}$	$1.127e^{3}$	4.051	------	$529.8e^{-6}$	$792.0e^{-3}$
24 hours	2.645	$399.3e^{-9}$	$1.3e^{3}$	1.488	------	$614.3e^{-6}$	$834.6e^{-3}$

Table 4. EIS fitting parameters of Sodium Alginate Ti substrates for Nyquist plot

Time Period	R_u (Ω)	Yo6	Alpha	W_D	R_{po} (Ω)
1 hour	5.255	195.4E-6	917.8E-3	15.35E-6	18.85E-3
3 hours	5.310	183.7E-6	923.9E-3	30.87E-6	9.743E-3
6 hours	5.328	169.2E-6	925.4E-3	19.70E-6	33.80E-3
12 hours	5.322	164.1.E-6	922.7E-3	11.546E-6	109.7E-3
24 hours	5.354	157.4E-6	933.0E-3	9.053E-6	27.24E-3

Table 5. Experimental and ANN predicted values for Open Circuit Potential for uncoated Ti and Biopolymer coated Titanium

Substrate condition		Substrate condition (Norm. value)	Time period (Hours)	Normalised value for time period	OCP values (Volts)	Normalised value for OCP	Predicted OCP values	Error
Uncoated Ti	1	0	1	0	-498.2	0.16179	0.16012	0.001664
	1	0	3	0.08696	-544.2	0.07002	0.07087	-0.00084
	1	0	6	0.21739	-579.3	0	0.01455	-0.01455
	1	0	12	0.47826	-551.4	0.05566	0.05567	-1.06E-05
	1	0	24	1	-557.3	0.04389	0.0451	-0.00121
Chitosan coated Titanium	2	0.3333	1	0	-258.2	0.64057	0.63479	0.005785
	2	0.3333	3	0.08696	-271	0.61504	0.56007	0.054963
	2	0.3333	6	0.21739	-322.1	0.5131	0.51361	-0.00051
	2	0.3333	12	0.47826	-329	0.49933	0.4994	-6.84E-05
	2	0.3333	24	1	-334.2	0.48896	0.48886	9.41E-05
Gelatin coated Titanium	3	0.6666	1	0	-415.9	0.32597	0.25842	0.067554
	3	0.6666	3	0.08696	-493.4	0.17136	0.18553	-0.01417
	3	0.6666	6	0.21739	-507.8	0.14264	0.1445	-0.00186
	3	0.6666	12	0.47826	-511.5	0.13526	0.13541	-0.00015
	3	0.6666	24	1	-513	0.13226	0.13245	-0.00018
Alginate coated Titanium	4	1	1	0	-78.03	1	1.02958	-0.02958
	4	1	3	0.08696	-80.94	0.95973	0.95815	0.00158
	4	1	6	0.21739	-115.6	0.92505	0.91156	0.013489
	4	1	12	0.47826	-137.5	0.88136	0.88073	0.00063
	4	1	24	1	-150.9	0.85463	0.85477	-0.00014